

1

Introduction

Chunhui Huang and Zuqiang Bian

*College of Chemistry and Molecular Engineering, Peking University, Beijing, 100871, P.R. China.
Email: chhuang@pku.edu.cn and bianzq@pku.edu.cn*

Lanthanide elements (referred to as Ln) have atomic numbers that range from 57 to 71. They are lanthanum (La), cerium (Ce), praseodymium (Pr), neodymium (Nd), promethium (Pm), samarium (Sm), europium (Eu), gadolinium (Gd), terbium (Tb), dysprosium (Dy), holmium (Ho), erbium (Er), thulium (Tm), ytterbium (Yb), and lutetium (Lu). With the inclusion of scandium (Sc) and yttrium (Y), which are in the same subgroup, this total of 17 elements are referred to as the rare earth elements (RE). They are similar in some aspects but very different in many others. Based on the electronic configuration of the rare earth elements, in this chapter we will discuss the lanthanide contraction phenomenon and the consequential effects on the chemical and physical properties of these elements. The coordination chemistry of lanthanide complexes containing small inorganic ligands is also briefly introduced here [1–5].

1.1 Electronic Configuration of Lanthanide Atoms in the Ground State

The electronic configuration of an atom in the ground state is determined by its principal quantum number n and angular quantum number l . According to the principle of lowest energy, there are two types of electronic configurations for the lanthanide elements: $[\text{Xe}]4f^n6s^2$ and $[\text{Xe}]4f^{n-1}5d^16s^2$. Here $[\text{Xe}]$ represents the electronic configuration of xenon, which is $1s^22s^22p^63s^23p^63d^{10}4s^24p^64d^{10}5s^25p^6$, where n represents a number from 1 to 14. Lanthanum, cerium, and gadolinium belong to the $[\text{Xe}]4f^n6s^2$ type, while praseodymium, neodymium, promethium, samarium, europium, terbium, dysprosium, holmium, erbium, thulium, ytterbium, and lutetium belong to the $[\text{Xe}]4f^{n-1}5d^16s^2$ type. Scandium and yttrium do not have 4f electrons but they do have similar chemical properties to lanthanide elements, because their outermost electrons have the $(n-1)d^1ns^2$ configuration. For this reason, they are generally regarded as being lanthanide elements.

Lanthanide elements adopt either the $[\text{Xe}]4f^n6s^2$ or $[\text{Xe}]4f^{n-1}5d^16s^2$ configuration depending on the relative energy level of these two electronic configurations. Figure 1.1 shows the

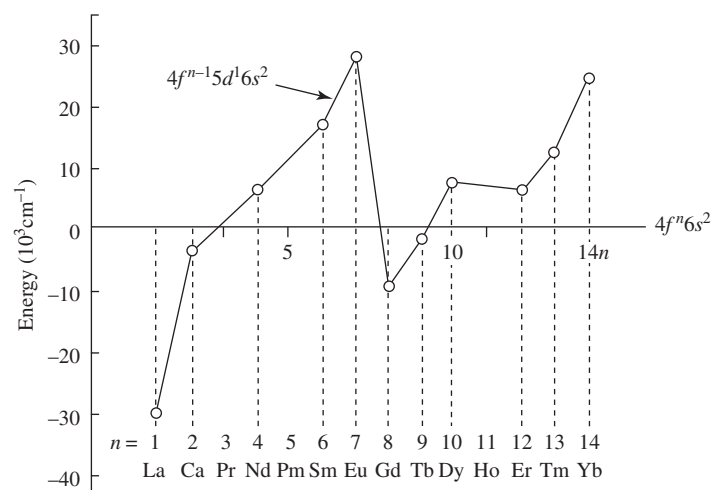


Figure 1.1 The relative energy level of the different electronic configurations, $4f^n 6s^2$ or $4f^{n-1} 5d^1 6s^2$ of neutral lanthanide atoms [5].

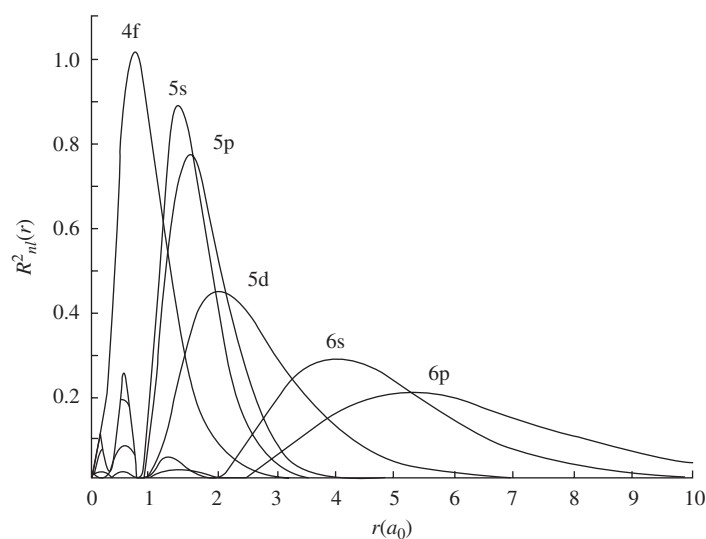
relative energy level of the neutral lanthanide atoms in the $4f^n 6s^2$ or $4f^{n-1} 5d^1 6s^2$ electronic configurations. For lanthanum, cerium, and gadolinium, the $[\text{Xe}]4f^{n-1} 5d^1 6s^2$ configuration is lower in energy than the $[\text{Xe}]4f^n 6s^2$ configuration, therefore, they adopt the former configuration. For terbium, the two configurations $[\text{Xe}]4f^9 6s^2$ and $[\text{Xe}]4f^8 5d^1 6s^2$ are energetically close to each other so terbium can adopt either one. Lutetium has 14 4f electrons and therefore its only possible configuration is $[\text{Xe}]4f^{14} 6s^2$. The other elements all have a $[\text{Xe}]4f^n 6s^2$ configuration. All the electronic configurations of lanthanide elements are summarized in Table 1.1.

1.2 Lanthanide Contraction

For multi-electron atoms a decrease in atomic radius, brought about by an increase in nuclear charge, is partially offset by increasing electrostatic repulsion among the electrons. The shielding effect originates from the inner electrons and decreases according to: $s > p > d > f$. For lanthanide elements, as the atomic number increases an electron is not added to the outermost shell but rather to the inner 4f shell (Table 1.1). Because of their diffusive property, 4f electrons do not all distribute within the inner part of the 5s5p shell and this can be clearly seen in Figures 1.2 and 1.3. Figure 1.2 shows the radial distribution functions of 4f, 5s, 5p, 5d, 6s, and 6p electrons for cerium and Figure 1.3 illustrates the radial distribution functions of 4f, 5s, 5p electrons for Pr^{3+} . An increase in 4f electrons only partly shields the increase in nuclear charge. It is generally believed that the screening constant of 4f electrons in trivalent lanthanide ions is about 0.85. The 4f electron clouds in neutral atoms are not as diffusive as in trivalent lanthanide ions and the screening constant of 4f electrons is larger but still less than one. Therefore, as the atomic number increases the effective attraction between the nucleus and the outer electrons increases. This increased attraction causes shrinkage in the atomic or ionic radius. This phenomenon is referred to as “lanthanide contraction.”

Table 1.1 The electronic configurations of lanthanide elements.

Z	Element		Electronic configurations of neutral atoms					Electronic configurations of trivalent ions	Atomic radius (pm) (coordination number = 12)	Atomic weight
			4f	5s	5p	5d	6s			
57	La	The inner orbitals have been full-filled, 46 electrons in all	0	2	6	1	2	[Xe]4f ⁰	187.91	138.91
58	Ce		1	2	6	1	2	[Xe]4f ¹	182.47	140.12
59	Pr		3	2	6		2	[Xe]4f ²	182.80	140.91
60	Nd		4	2	6		2	[Xe]4f ³	182.14	144.24
61	Pm		5	2	6		2	[Xe]4f ⁴	(181.0)	(147)
62	Sm		6	2	6		2	[Xe]4f ⁵	180.41	150.36
63	Eu		7	2	6		2	[Xe]4f ⁶	204.20	151.96
64	Gd		7	2	6	1	2	[Xe]4f ⁷	180.13	157.25
65	Tb		9	2	6		2	[Xe]4f ⁸	178.33	158.93
66	Dy		10	2	6		2	[Xe]4f ⁹	177.40	162.50
67	Ho		11	2	6		2	[Xe]4f ¹⁰	176.61	164.93
68	Er		12	2	6		2	[Xe]4f ¹¹	175.66	167.26
69	Tm		13	2	6		2	[Xe]4f ¹²	174.62	168.93
70	Yb		14	2	6		2	[Xe]4f ¹³	193.92	173.04
71	Lu		14	2	6	1	2	[Xe]4f ¹⁴	173.49	174.97
			3d	4s	4p	4d	5s			
21	Sc	Inner 18 electrons	1	2				[Ar]	164.06	44.956
39	Y		10	2	6	1	2	[Kr]	180.12	88.906

**Figure 1.2** Radial distribution functions of 4f, 5s, 5p, 5d, 6s, and 6p electrons for cerium [2]. (Courtesy of Z.B. Goldschmidt, “Atomic properties (free atom),” in K.A. Gschneidner and L. Eyring (eds.), *Handbook on the Physics and Chemistry of Rare Earths*, volume I, 2nd edition, North Holland Publishing Company, Amsterdam. © 1978.)

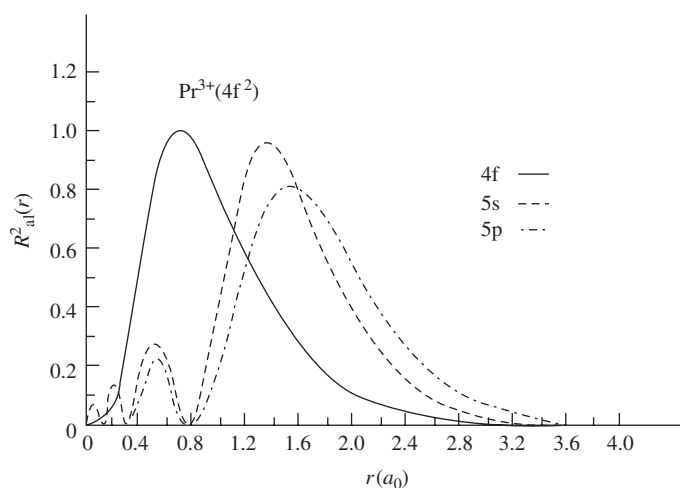


Figure 1.3 Radial distribution functions of 4f, 5s, 5p electrons for Pr^{3+} [6]. (With kind permission from Springer Science + Business Media: *Organometallics of the f Element*, © 1979, p. 38, T.J. Marks, and R.D. Fisher, figure 1, D. Reidel Publishing Company, Dordrecht.)

One effect of lanthanide contraction is that the radius of trivalent yttrium ion (Y^{3+}) is measured to be between that of Ho^{3+} and Er^{3+} , and the atomic radius of yttrium is between neodymium and samarium. This results in the chemical properties of yttrium being very similar to those of lanthanide elements. Yttrium is often found with lanthanide elements in natural minerals. The chemical properties of yttrium may be similar to the lighter or the heavier lanthanide elements in different systems and this depends on the level of covalent character of the chemical bonds in those systems.

Another effect of lanthanide contraction is that the third row of the d-block elements have only marginally larger atomic radii than the second transition series. For example, zirconium and hafnium, niobium and tantalum, or tungsten and molybdenum have similar ionic radii and chemical properties (Zr^{4+} 80 pm, Hf^{4+} 81 pm; Nb^{5+} 70 pm, Ta^{5+} 73 pm; Mo^{6+} 62 pm, W^{6+} 65 pm). These elements are also found in the same natural minerals and are difficult to separate.

Because of lanthanide contraction, the radius of lanthanide ions decreases gradually as the atomic number increases, resulting in regular changes in the properties of lanthanide elements as the atomic number increases. For example, the stability constant of lanthanide complexes usually increases as the atomic number increases; the alkalinity of lanthanide ions decreases as the atomic number increases; the pH at which hydrates start to precipitate from an aqueous solution decreases gradually as the atomic number increases.

Because of lanthanide contraction, the radius of lanthanide atoms also changes regularly. Because the shielding effect of 4f electrons in lanthanide atoms is not so strong as those in lanthanide ions, lanthanide contraction is weaker in lanthanide atoms than in ions. The atomic radius of a hexagonal crystal metal is defined as the average distance between adjacent atoms in a close-packed plane and in an adjacent close-packed plane (Table 1.1). The relationship between ionic radius and atomic number is shown in Figure 1.4. The atomic radius also exhibits lanthanide contraction, except for cerium, europium, and ytterbium. However, the contraction of lanthanide atoms is not so prominent as that of lanthanide ions (Figure 1.5).

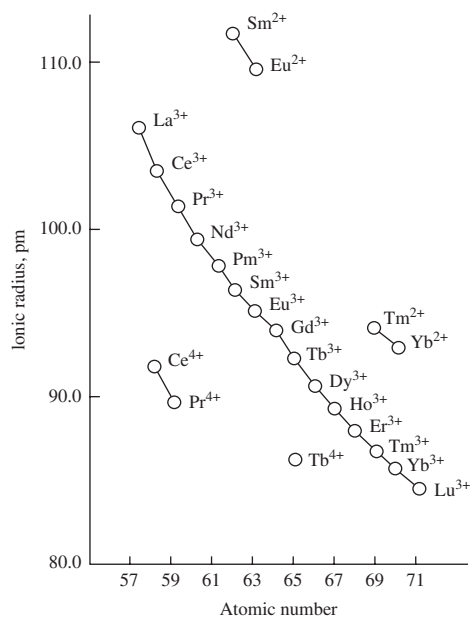


Figure 1.4 The relationship between ionic radius and atomic number of lanthanide ions [1, 5].

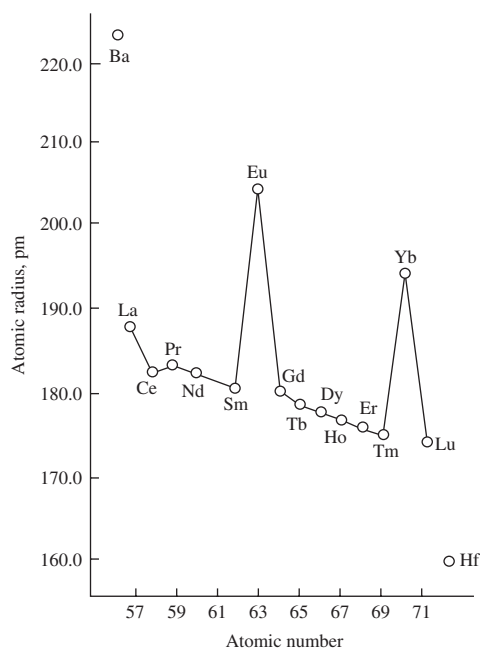


Figure 1.5 The relationship between atomic radius and atomic number of lanthanide atoms [1, 5].

The abnormal behavior for the atomic radii of cerium, europium, and ytterbium can be explained as follows. The atomic radius of a metal approximately equals the radius of the maxima of the outermost electron cloud density. Therefore, the outermost electron clouds overlap in metals. These electrons can move freely in the crystal lattice and become conducting electrons. Generally speaking, there are three conducting electrons in lanthanide metals. Europium and ytterbium tend to maintain a $4f^7$ and $4f^{14}$ electron configuration, respectively, and thus they provide only two conducting electrons. The overlapping part of the outermost electrons between adjacent atoms becomes smaller and the atomic radius becomes larger. On the contrary, a cerium atom has only one $4f$ electron and it tends to provide four conducting electrons to obtain a stable electronic configuration. The overlapping part of the outermost electrons becomes larger, which causes the distance between adjacent atoms to become smaller compared with other lanthanide elements.

1.3 Specificity of the Photophysical Properties of Rare Earth Compounds

Because the $4f$ shells of lanthanide elements are unfilled, different arrangements of $4f$ electrons generate different energy levels. The $4f$ electron transitions, between the various energy levels, could generate numerous absorption and emission spectra.

Electronic configurations and spectral terms of ground state trivalent lanthanide ions are listed in Table 1.2. Figure 1.6 shows the energy level diagram for trivalent lanthanide ions.

Table 1.2 Electronic configurations and spectral terms of trivalent lanthanide ions in the ground state [5].

Ion	4f ^a	Magnetic quantum number of 4f orbital							L	S	J	Ground state spectral term	Δ (cm ⁻¹)	ζ _{4f} (cm ⁻¹)
		3	2	1	0	-1	-2	-3						
J = L - S														
La ³⁺	0								0	0	0	¹ S ₀		
Ce ³⁺	1	↑							3	1/2	5/2	² F _{5/2}	2200	640
Pr ³⁺	2	↑	↑						5	1	4	³ H ₄	2150	750
Nd ³⁺	3	↑	↑	↑					6	3/2	9/2	⁴ I _{9/2}	1900	900
Pm ³⁺	4	↑	↑	↑	↑				6	2	4	⁵ I ₄	1600	1070
Sm ³⁺	5	↑	↑	↑	↑	↑			5	5/2	5/2	⁶ H _{5/2}	1000	1200
Eu ³⁺	6	↑	↑	↑	↑	↑	↑		3	3	0	⁷ F ₀	350	1320
J = L + S														
Gd ³⁺	7	↑	↑	↑	↑	↑	↑	↑	0	7/2	7/2	⁸ S _{7/2}		1620
Tb ³⁺	8	↑↓	↑	↑	↑	↑	↑	↑	3	3	6	⁷ F ₆	2000	1700
Dy ³⁺	9	↑↓	↑↓	↑	↑	↑	↑	↑	5	5/2	15/2	⁶ H _{15/2}	3300	1900
Ho ³⁺	10	↑↓	↑↓	↑↓	↑	↑	↑	↑	6	2	8	⁵ I ₈	5200	2160
Er ³⁺	11	↑↓	↑↓	↑↓	↑↓	↑	↑	↑	6	3/2	15/2	⁴ I _{15/2}	6500	2440
Tm ³⁺	12	↑↓	↑↓	↑↓	↑↓	↑↓	↑	↑	5	1	6	³ H ₆	8300	2640
Yb ³⁺	13	↑↓	↑↓	↑↓	↑↓	↑↓	↑↓	↑	3	1/2	7/2	² F _{7/2}	10 300	2880
Lu ³⁺	14	↑↓	↑↓	↑↓	↑↓	↑↓	↑↓	↑↓	0	0	0	¹ S ₀		

^aThe number of $4f$ electrons



1.3.1 Spectral Terms

There are four quantum numbers for describing the state of an electron, they are: principal quantum number n , which takes the value of 1, 2, 3, 4, ...; azimuthal quantum number, or orbital quantum number l , which takes the value of 0, 1, 2, 3, ..., $n - 1$; the magnetic quantum number m_l , which takes the value of 0, ± 1 , ± 2 , ± 3 ... $\pm l$; and the spin quantum

number s , which takes the value of $1/2$; also, m_s is the spin magnetic quantum number. In addition, the electron in an atom has its spin movement, while also moving around the orbital. To describe this state, the overall angular quantum number, j was introduced. This is the vector sum momentum of l and s , that is, $j = l + s, l + s - 1, \dots, |l - s|$. m_j is the angular magnetic quantum number j along the magnetic field.

In a multi-electronic atom, the following quantum numbers can also be used to describe the energy levels, and the relationships between the quantum number of electrons are as follows.

1. Total spin quantum number $S = \sum m_s$.
2. Total orbital quantum number $L = \sum m_l$.
3. Total magnetic orbital quantum number M_L .
4. Total angular momentum quantum number J , which takes $L + S, L + S - 1, \dots, L - S$ when $L \geq S$, and can take $S + L, S + L - 1, \dots, S - L$ when $L \leq S$. M_J is the total magnetic angular quantum number J along the magnetic field.

The spectral term is a symbol which combines the azimuthal quantum number l and magnetic quantum number m to describe the energy level relationship between electronic configurations.

Seven orbitals are present in the 4f shell ($l = 3$). Their magnetic quantum numbers are $-3, -2, -1, 0, 1, 2$, and 3 , respectively. When lanthanide elements are in their ground states, the distribution of the 4f electrons in the orbitals are as shown in Table 1.2. Here, Δ represents the energy difference between the ground state and the J multiple state that lies right above the ground state; ζ_{4f} is the spin-orbital coupling coefficient.

In this table, M_L is the total magnetic quantum number of the ion. Its maximum is the total orbital angular quantum number L . M_s is the total spin quantum number along the magnetic field direction. Its maximum is the total spin quantum number S . $J = L \pm S$, is the total angular momentum quantum number of the ion and is the sum of the orbital and spin momentum. For the first seven ions (from La^{3+} to Eu^{3+}), $J = L - S$; for the last eight ions (from Gd^{3+} to Lu^{3+}), $J = L + S$. The spectral term consists of three quantum numbers, L , S , and J and may be expressed as $^{2S+1}L_J$. The value of L is indicated by S, P, D, F, G, H, and I for $L = 0, 1, 2, 3, 4, 5$, and 6 , respectively. The number on the top left represents the multiplicity of the spectral term. It equals $2S + 1$. The number on the bottom right is the total angular momentum quantum number J . Take Nd^{3+} as an example, $L = 6$ and its corresponding capital letter is I; $S = 3/2$ (three uncoupled electrons) so $2S + 1 = 4$; $J = L - S = 6 - 3/2 = 9/2$. Therefore, the spectral term for the ground state of Nd^{3+} is $^4\text{I}_{9/2}$.

1.3.2 Selection Rules for Atomic Spectra

The 4f electrons of lanthanide elements can be placed in any 4f orbital except for La^{3+} (empty) and Lu^{3+} (full) and this results in various spectral terms and energy levels for lanthanide elements. For example, praseodymium has 41 energy levels at the $4f^3, 6s^2$ configuration, 500 energy levels at the $4f^3, 6s^1, 6p^1$ configuration, 100 energy levels at the $4f^2, 5d^1, 6s^2$ configuration, 750 energy levels at the $4f^3, 5d^1, 6s^1$ configuration, and 1700 energy levels at the $4f^3, 5d^2$ configuration. Gadolinium has 3106 energy levels at the $4f^7, 5d^1, 6s^2$ configuration while its excited state $4f^7, 5d^1, 6s^1, 6p^1$ has as many as 36 000 energy levels. However, because of selection rule constraints many transitions between different energy levels are forbidden

transitions and the number of visible spectral lines is far less than expected. Experimental data, which has subsequently been proved by quantum mechanical theory, shows that only transitions that satisfy the following rules are allowed:

1. For $L - S$ coupling (so-called Russell–Saunders coupling), which is to combine the s of every electron to get S , and combine the l of every electron to obtain L initially and finally to combine S and L to get J :

$$\Delta S = 0$$

$$\Delta L = \pm 1$$

$$\Delta J = 0, \pm 1, \text{ (except } 0 \rightarrow 0)$$

$$\Delta M_J = 0, \pm 1 \text{ (for } \Delta J = 0, \text{ except } 0 \rightarrow 0)$$
2. For $j-j$ coupling, which is firstly to combine s and l for every electron to obtain j , and then get the total angular quantum number J through $j-j$ coupling:

$$\Delta j = 0, \pm 1 \text{ (for the transition electron only), } \Delta j = 0 \text{ (for the rest of the electrons)}$$

$$\Delta J = 0, \pm 1, \text{ (except } 0 \rightarrow 0)$$

$$\Delta M_J = 0, \pm 1, \text{ (for } \Delta J = 0, \text{ except } 0 \rightarrow 0)$$

In general, lanthanide atoms or ions with an unfilled 4f shell have about 30 000 visible spectral lines. Transition metals with an unfilled 5d shell have about 7000 visible spectral lines. Main group elements with an unfilled p shell only have about 1000 visible spectral lines. Lanthanide elements, therefore, have more electronic energy levels and spectral lines than the more common elements. They can absorb electromagnetic waves from the ultraviolet to the infrared and emit their characteristic spectra.

1.3.3 Lifetime

The lifetime (τ) of an excited state is an important term when the kinetic process is of concern. The lifetime of an excited molecule is not a time measuring the existence of the excited state but is rather the deactivation time needed for excited states to reduce to 1/e of its initial population. It is defined as follows:

$$\tau = 1 / \Sigma k_f \quad (1.1)$$

where k_f is the rate constant of deactivation and Σk_f is the sum of all the rate constants of the deactivation processes, including radiative and non-radiative processes in the system.

Another characteristic of lanthanide elements is that some excited states have very long lifetimes ($10^{-2} \sim 10^{-6}$ s) while the average lifetimes of other typical atoms or ions range from 10^{-8} to 10^{-10} s. These long lifetime excited states are referred to as metastable states. These metastable states of lanthanide elements are caused by $4f \rightarrow 4f$ electronic transitions. According to the selection rules, these $\Delta l = 0$ electric dipole transitions are forbidden but are in fact observed. There are two major reasons for the forbidden transitions occurring: mixing between 4f configurations of opposite parity and the deviation of symmetry from an inversion center. Because lanthanide elements have many $4f \rightarrow 4f$ transitions between metastable states, the excited states of lanthanide elements have long lifetimes. This enables some lanthanide materials to be used in laser and fluorescence materials.

1.3.4 Absorption Spectra

In lanthanide elements, the $5s^2$ and $5p^6$ shells are on the outside of the $4f$ shell. The $5s^2$ and $5p^6$ electrons are shielded, any force field (the crystal field or coordinating field in crystals or complexes) of the surrounding elements in complexes have little effect on the electrons in the $4f$ shell of the lanthanide elements. Therefore, the absorption spectra of lanthanide compounds are line-like spectra similar to those of free ions. This is different from the absorption spectra of d-block compounds. In d-block compounds, spectra originate from $3d \rightarrow 3d$ transitions. The nd shell is on the outside of the atoms so no shielding effect exists. Therefore, the $3d$ electrons are easily affected by crystal or coordinating fields. As a result, d-block elements show different absorption spectra in different compounds. Because of a shift in the spectrum line in the d-block, absorption spectra change from line spectra in free ions to band spectra in compounds.

Most trivalent rare earth ions have no or very weak absorption in the visible range [8]. For example, Y^{3+} , La^{3+} , Gd^{3+} , Yb^{3+} , and Lu^{3+} in inorganic acid aqueous solutions are colorless. It is worth noting that colors of the aqueous solutions for ions having the $4f^n$ electronic configuration are usually similar to those that have the $4f^{14-n}$ configuration (Figure 1.7).

Another characteristic of rare earth ions (except for Ce^{3+} and Yb^{3+}) in absorption spectra are their linear-like behavior. This comes from f–f transitions where $4f$ electrons exchange between different $4f$ energy levels. However, no f–f transition is allowed for $Ce^{3+}(4f^1)$ or $Yb^{3+}(4f^{13})$. The broad absorption bands observed originates from configuration transitions, for example $4f^n$ to $4f^{n-1}5d^1$.

f–f transitions of lanthanide ions can be divided into magnetic dipole transitions and electric dipole transitions. In some cases an electric multi-dipole transition is also observed. According to the classic transition selection rule, a transition is forbidden when $\Delta L = 0$, that is, the f–f electric dipole transition is forbidden. However, it has been observed experimentally and this is because an odd parity term or an anti-parity electron is introduced into the $4f^n$ configuration to some extent.

The absorption spectra of rare earth complexes are mainly determined by the coordinated organic ligands.

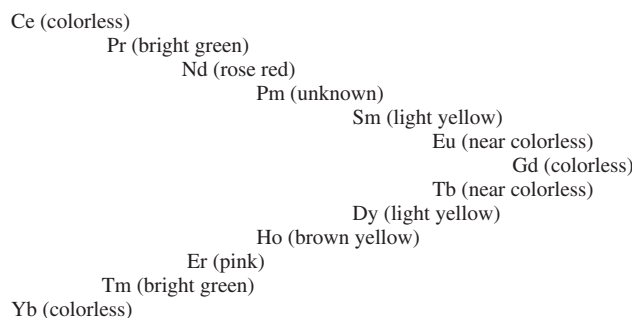


Figure 1.7 Similarity in color between ions with the electron configurations $4f^n$ and $4f^{14-n}$.

1.3.5 The Emission Spectra of Rare Earth Compounds

In the 1940s, emissions from rare earth complexes were observed and research into this phenomenon has received growing and lasting attention because of their potential application in optical communications, new generation displays, and sensors.

Since the dipole strength of f - f transitions are formally forbidden, typically, these extinction coefficients are of the order of $1 \text{ M}^{-1}\text{cm}^{-1}$, an alternative path has to be used which is called luminescence sensitization or antenna effect, that is when the luminescent ion is coordinated with an organic ligand or imbedded into a matrix, then the energy absorbed will be transferred from the surrounding onto the luminescent ion and subsequently the ion emits characteristic light.

To quantitatively describe the effect of the emission, quantum yield Q is introduced, which has the following definition:

$$Q = \frac{\text{number of emitted photons}}{\text{number of absorbed photons}} \quad (1.2)$$

According to the emission properties, rare earth complexes can be divided into four groups as follows:

1. $\text{Sm}^{3+}(4f^5)$, $\text{Eu}^{3+}(4f^6)$, $\text{Tb}^{3+}(4f^8)$ and $\text{Dy}^{3+}(4f^9)$;
2. $\text{Pr}^{3+}(4f^2)$, $\text{Nd}^{3+}(4f^3)$, $\text{Ho}^{3+}(4f^{10})$, $\text{Er}^{3+}(4f^{11})$, $\text{Tm}^{3+}(4f^{12})$ and $\text{Yb}^{3+}(4f^{13})$;
3. $\text{Sm}^{2+}(4f^6)$, $\text{Eu}^{2+}(4f^7)$, $\text{Yb}^{2+}(4f^{14})$ and $\text{Ce}^{3+}(4f^1)$;
4. $\text{Sc}^{3+}(4f^0)$, $\text{Y}^{3+}(4f^0)$, $\text{La}^{3+}(4f^0)$, $\text{Gd}^{3+}(4f^7)$ and $\text{Lu}^{3+}(4f^{14})$.

For the first group, emissions originate because of the transition of $4f$ electrons from the lowest excited states to the ground states and the emissions are in the visible region. The probabilities of these transitions are relatively high and strong emissions may be observed. The lifetimes of these emissions are in the microsecond or milliseconds scale. For the second group, the energy levels of these ions are very close to one another. Thus, the emissions are often in the infrared region and their intensities are weaker than those of the first group by several orders of magnitude. All the ions in the third group exist in lower oxidation states and their emissions originate from d - f transitions and not f - f transitions, which would show broader emission bands. Obviously, the ions in the last group all have so-called stable electronic configurations, that is, their $4f$ orbitals are either "empty," "half-filled" or "all-filled." Therefore, no f - f transitions occur except in gadolinium complexes, which emit in the ultraviolet region. However, these complexes do sometimes emit when suitable ligands are coordinated to the central ions. In these cases, the emissions are caused by ligand emission complexes.

In 1990, Buono-core suggested a simplified diagram to show the three different mechanisms for intra-molecular energy transition in lanthanide complexes (Figure 1.8).

In Figure 1.8a, the ligands of the complex are excited from their ground state (S_0) to their excited singlet state (S_1) by the absorption of light energy. Energy is then transferred to the excited triplet state (T_1) through intersystem crossing. The energy could then transfer to the rare earth ion if the energy levels match each other and the electrons of the central ions can thus become excited. When the electrons return from the excited state to the ground state the complex emits with the characteristic wavelength of the central ion. In the case of Figure 1.8b, the ligands of the complex are excited from S_0 to S_1 and from there the energy absorbed could be transferred to the central ion directly but not through the T_1 state. In the case of Figure 1.8c, the ligands of the complex are excited from S_0 to S_1 and then the energy

absorbed can be transferred back and forth between S_1 and T_1 and then to the excited states, multiply, and finally transfer to the rare earth ion to excite it and then they return to the ground state. The complexes can then emit their characteristic emissions. Therefore, the theoretical emission yield is 100%.

It has been very difficult to unambiguously prove which state is responsible for the energy transfer processes because of the lack of information regarding the emission from the excited states of the coordinated ligand and the difficulties in determining ligand-localized triplet–triplet absorption spectra of lanthanide complexes. All the experimental work conducted seemed to support case (a) in Figure 1.8.

In 2004, Zhang and coworkers reported the first experimentally observed example of case (b) in Figure 1.8 by means of time-resolved luminescence spectroscopy with the system shown in Figure 1.9.

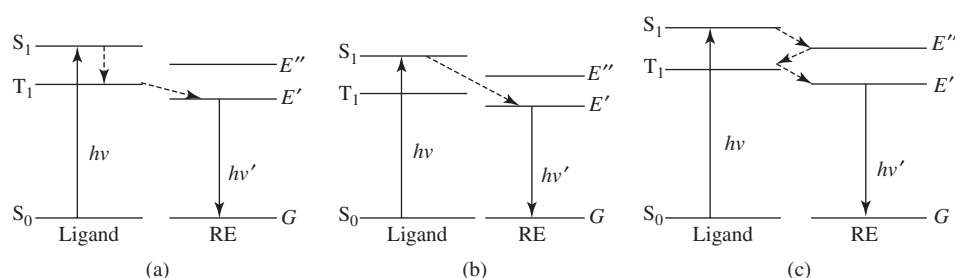


Figure 1.8 Three possible intra-molecular energy transition mechanisms [9]. (Reprinted from *Coordination Chemistry Reviews*, **99**, G.E. Buono-core, H. Li, and B. Marciniak, “Quenching of excited states by lanthanide ions and chelates in solution,” 55–87, 1990, with permission from Elsevier.)

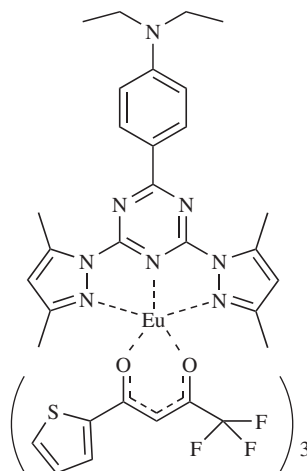


Figure 1.9 The molecular formula of $\text{Eu}(\text{tta})_3\text{L}$, $\text{L} = 4$ -[4, 6-bis(3, 5-dimethyl-1H-pyrazol-yl)-1, 3, 5-triazin-2-yl]-N,N-diethylbenzenamine, $\text{tta} = 2$ -thenoyltrifluoroacetate [10]. (Reprinted with permission from C. Yang, L.M. Fu, Y. Wang, Y. *et al.*, “Highly luminescent europium complex showing visible-light-sensitized red emission: Direct observation of the singlet pathway,” *Angewandte Chemie International Edition*, 2004, **43**, 5010–5013. © Wiley-VCH Verlag GmbH & Co. KGaA.)

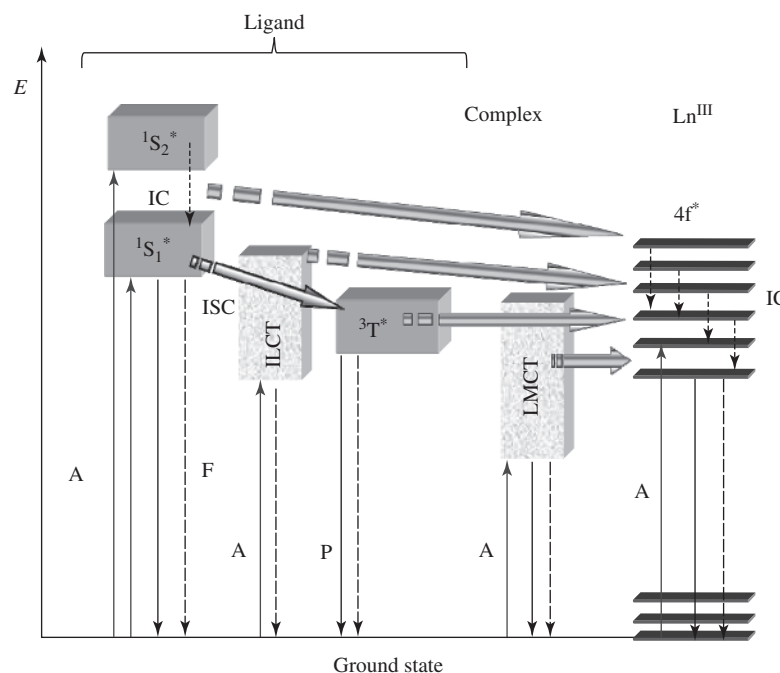


Figure 1.10 Schematic representation of energy absorption, migration, emission (solid arrows), and dissipation (dashed arrows) processes in a lanthanide complex. $1S^*$ or S = singlet state, $3T^*$ or T = triplet state, A = absorption, F = fluorescence, P = phosphorescence, IC = internal conversion, ISC = intersystem crossing, ILCT (or IL) = intra-ligand charge transfer, LMCT (or LM) = ligand-to-metal charge transfer. Back transfer processes are not drawn for the sake of clarity [11]. (Adapted with permission from Bünzli, J. C. G. and Eliseeva, S. V., “Basics of lanthanide photophysics,” in P. Hänninen and H. Härmä (eds.), *Springer Series on Fluorescence*, **7**, Lanthanide Spectroscopy, Materials and Bio-Applications, © 2010, Springer-Verlag, Berlin.)

However, over the past ten years the situation has actually been found to be much more complicated. Bünzli summarized recent progress and proposed the diagram shown in Figure 1.10. In these cases, the complexes contain aromatic unsaturated ligands where they display a large energy absorption cross section and the energy is not usually transferred directly onto the emitting state, particularly in the case of a europium complex for which the 0–0 transition is strictly forbidden. In these processes, metal to ligand charge transfer (MLCT) and/or intra-ligand charge transfer (ILCT), even the triplet metal to ligand charge transfer ($^3\text{MLCT}$, where M stands for transition metals in a hetero-nuclear complex) may also emerge as important players.

1.4 Specificities of Rare Earth Coordination Chemistry

Rare earth coordination chemistry has many characteristic properties compared with d-block metal complexes. Four main issues will be discussed in this section: the valence state, chemical bonding, the coordination number, and the tetra effect – the changing gradation rules in rare earth coordination chemistry.

1.4.1 Valence State of Rare Earth Elements

Rare earth elements have similar configurations in the two outermost shells. They exhibit typical metallic properties in chemical reactions. They tend to lose three electrons and exhibit a 3+ valence state. From the Periodic Table of the elements, rare earth elements are classed as less reactive than alkali metals and alkaline earth metals but more reactive than other metals. They should be stored in an inert liquid otherwise they will be oxidized and lose their metal luster. The metal reactivity increases gradually from scandium to lanthanum and decreases gradually from lanthanum to lutetium. That is to say, lanthanum is the most reactive metal of the 17 rare earth elements. Rare earth metals can react with water and release hydrogen. They react more vigorously with acids but do not react with bases.

According to Hund's rule, electron shells are stable when empty, full or half-full. For example, the configurations $4f^0$ (La^{3+}), $4f^7$ (Gd^{3+}), and $4f^{14}$ (Lu^{3+}) are stable. Ce^{3+} , Pr^{3+} , and Tb^{3+} have one or two more electrons than required for stable electronic configurations so they can be further oxidized to a 4+ state. In contrast, Sm^{3+} , Eu^{3+} , and Yb^{3+} have one or two less electrons than required for a stable electronic configuration and they, therefore, tend to receive one or two electrons and undergo a reduction to a 2+ state. These are the reasons for these elements having abnormal valence states.

Standard reduction potentials, $E_{\text{Ln}^{4+}/\text{Ln}^{3+}}^\circ$ and $E_{\text{Ln}^{3+}/\text{Ln}^{2+}}^\circ$, represent the driving force stability of the reduction state. The more positive the value of E_{red}° , the greater the driving force for reduction. The standard reduction potentials of rare earths are shown in Table 1.3.

Table 1.3 Standard reduction potentials E_{red}° of rare earths.

Electro-pair	$E^\circ(\text{V})$	Electro-pair	$E^\circ(\text{V})$
$\text{Ce}^{4+}/\text{Ce}^{3+}$	+1.74	$\text{Eu}^{3+}/\text{Eu}^{2+}$	-0.35
$\text{Tb}^{4+}/\text{Tb}^{3+}$	+3.1 \pm 0.2	$\text{Yb}^{3+}/\text{Yb}^{2+}$	-1.15
$\text{Pr}^{4+}/\text{Pr}^{3+}$	+3.2 \pm 0.2	$\text{Sm}^{3+}/\text{Sm}^{2+}$	-1.55
$\text{Nd}^{4+}/\text{Nd}^{3+}$	+5.0 \pm 0.4	$\text{Tm}^{3+}/\text{Tm}^{2+}$	-2.3 \pm 0.2
$\text{Dy}^{4+}/\text{Dy}^{3+}$	+5.2 \pm 0.4		

The data shown in the table indicate that when comparing $E_{\text{Ce}^{4+}/\text{Ce}^{3+}}^\circ$ with $E_{\text{Tb}^{4+}/\text{Tb}^{3+}}^\circ$ electronic pairs, to act as an oxidizing agent, Tb^{4+} is stronger than Ce^{4+} ; to act as a reducing agent Ce^{3+} is stronger than Tb^{3+} . When comparing $E_{\text{Eu}^{3+}/\text{Eu}^{2+}}^\circ$ with $E_{\text{Yb}^{3+}/\text{Yb}^{2+}}^\circ$, to act an oxidizing agent Yb^{2+} is stronger than Eu^{2+} under the standard conditions. Figure 1.11 visualizes this

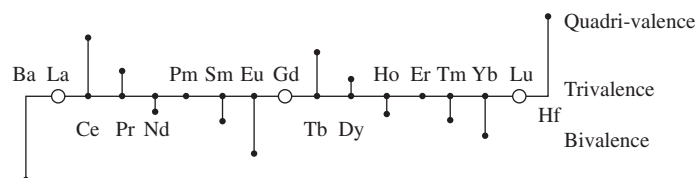


Figure 1.11 Valence states of lanthanide elements.

trend. The transverse axis is the atomic number and the length of the short lines along the vertical axis represents the trend of valence state variation.

1.4.2 Chemical Bonding of Rare Earth Elements

As a group of typical metal elements, lanthanide elements can form chemical bonds with most nonmetal elements. Some low-valence lanthanide elements can form chemical bonds in organometallic or atom cluster compounds. Because lanthanide elements lack sufficient electrons and show a strong repulsive force towards a positive charge, chemical bonds between lanthanide metals have not yet been observed. Table 1.4 shows that 1391 structure-characterized lanthanide complexes were reported in publications between 1935 and 1995 and these are sorted by chemical bond type.

From a soft–hard acid–base point of view, lanthanide elements are hard bases. Thus, they tend to form chemical bonds with atoms that belong to the hard acid group. For example, oxygen and lanthanide elements tend to form RE–O bonds. The data in Table 1.4 show that 1080 complexes (77.6% of the 1391 complexes) contain RE–O bonds. Among these, 587 complexes (42.2% of the 1391 complexes) contain RE–O bonds only. On the other hand, only 46 complexes contain RE–S bonds, 7 complexes contain RE–Se bonds, and 10 complexes contain RE–Te bonds. Lanthanide elements can also form chemical bonds with nitrogen group atoms. There are 318 lanthanide complexes that contain RE–N bonds and 15 complexes that contain RE–P bonds. No complex containing a RE–As bond has been observed yet. Lanthanide complexes containing RE–C bonds are not stable under normal conditions. However, 407 complexes containing RE–C bonds are stable under water-free conditions. Complexes containing RE–Si bonds are very rare.

The nature of chemical bonds in lanthanide complexes and whether 4f electrons contribute to bonding in these complexes has been a long and controversial problem. To further understand the electronic structure of lanthanide complexes, scientists have investigated the nature of their molecular bonding by quantum chemistry. It is now generally believed that chemical bonds in lanthanide complexes exhibit polar covalent bond properties and that 4f electrons do not contribute to bonding, with the major contribution being from the 5d and 6s orbitals, while the 4f orbital is highly localized [12].

1.4.3 Coordination Numbers of Rare Earth Complexes

1.4.3.1 Definition of Coordination Number

The coordination number is a well known concept. However, its definition is not standard. For example, the Cambridge database defines the coordination number of cyclopentadiene as one. It defines the coordination number as the number of ligands coordinated to a central atom. Cotton reported the coordination number of $(C_5H_5)_2ZrCl_2$ to be four, which also adopts this definition. However, the coordination numbers of butadiene and bipyridine are defined as two in some sources. This obviously conflicts with the former definition. Guangxian Xu defined the coordination number of the central atom to be the number of coordinating atoms for σ ligands or the number of π electron pairs provided by π ligands. According to this definition 2,6-xylene provides four σ coordinating atoms to the central lutetium atom in $[Li(THF)_4][Lu-(2,6-Me_2C_6H_3)_4]$ and the coordination number of Lu^{3+} is four. As another

Table 1.4 The chemical bonding of lanthanide complexes.

Chemical bond	Compound				Sum total
	Sc	Y	Ln	Subtotal	
RE–O	13	54	520	587	719
RE–N	1	1	25	27	
RE–C	4	6	64	74	
RE–L (L = halogen)	0	2	6	8	
RE–S	0	0	21	21	
RE–P	1	0	1	2	
RE–O, RE–N	5	13	183	201	412
RE–O, RE–C	1	15	92	108	
RE–O, RE–L	4	10	58	72	
RE–O, RE–S	0	0	17	17	
RE–O, RE–P	0	1	1	2	
RE–O, RE–H	0	4	3	7	
RE–O, RE–Te	0	0	3	3	
RE–O, RE–Si	0	0	1	1	
RE–O, RE–Ge	0	0	1	1	
RE–N, RE–C	4	7	40	51	64
RE–N, RE–L	0	1	5	6	
RE–N, RE–S	0	0	2	2	
RE–N, RE–P	0	0	1	1	
RE–N, RE–H	0	0	1	1	
RE–N, RE–Se	0	0	2	2	
RE–N, RE–Te	0	0	1	1	
RE–C, RE–L	2	6	58	66	109
RE–C, RE–P	0	0	5	5	
RE–C, RE–S	0	0	5	5	
RE–C, RE–H	2	9	12	23	
RE–C, RE–Te	0	0	2	2	
RE–C, RE–Se	0	0	2	2	
RE–C, RE–Si	0	0	2	2	
RE–L, RE–H	0	3	1	4	
RE–O, RE–N, RE–C	0	2	12	14	80
RE–O, RE–N, RE–P	0	0	1	1	
RE–O, RE–N, RE–L	0	1	5	6	
RE–O, RE–C, RE–L	1	2	39	42	
RE–O, RE–C, RE–H	0	5	5	10	
RE–O, RE–C, RE–Se	0	0	3	3	
RE–O, RE–C, RE–Te	0	0	3	3	
RE–O, RE–C, RE–S	0	0	1	1	
RE–N, RE–C, RE–P	0	1	0	1	2
RE–N, RE–C, RE–L	0	0	1	1	
RE–C, RE–L, RE–H	0	1	0	1	2
RE–C, RE–P, RE–Te	1	0	0	1	
RE–N, RE–C, RE–P, RE–H	1	0	0	1	3
RE–N, RE–C, RE–P, RE–Cl	0	1	0	1	
RE–N, RE–O, RE–C, RE–L	0	0	1	1	
					1391

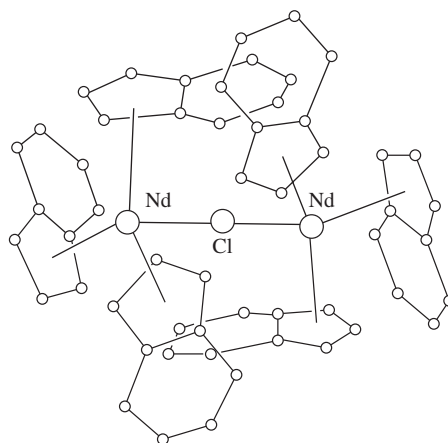


Figure 1.12 The structure of the anion in the complex $[\text{Nd}(\eta^5\text{-C}_9\text{H}_7)_3] (\mu_2\text{-Cl})\text{Nd}(\eta^5\text{-C}_9\text{H}_7)_3[\text{Na}(\text{THF})_6]$ [13]. (Adapted with permission from M.Q. Chen, G. Wu, Z. Huang, *et al.*, “Studies on rare earth-indenyl compounds. 2. Synthesis and crystal structure of hexakis(tetrahydrofuran)sodium (μ_2 -chloro)bis(triindenylneodymate),” *Organometallics*, **7**, no. 4, 802–806, 1988. © 1988 American Chemical Society.)

example, $\text{Ce}(\text{C}_9\text{H}_7)_3\text{Py}$ (C_9H_7 represents indene, Py represents pyridine) has an X-ray single crystal structure which shows that every indene ligand provides three pairs of π electrons and, therefore, the coordination number of Ce^{3+} in this complex is ten. According to this definition, the coordination numbers contributed by the π ligands $\text{CH}_2=\text{CH}_2$, $\text{CH}_2=\text{CH}-\text{CH}=\text{CH}_2$, C_6H_6 , C_5H_5^- , and $(\text{C}_8\text{H}_8)^{2-}$ are one, two, three, three, and five, respectively. In $[\text{Ce}(\text{C}_8\text{H}_8)_2]^-$, C_8H_8 has a planar structure and according to the $4n+2$ rule, only those annular structures that have 6, 10, 14, or 18 π electrons are aromatic. When C_8H_8 exists as an anion, it has ten π electrons and it can provide the central atom with five pairs of π coordinating electrons. Therefore, the coordination number of cerium in $[\text{Ce}(\text{C}_8\text{H}_8)_2]^-$ is ten. In the complex $[\text{Nd}(\eta^5\text{-C}_9\text{H}_7)_3] (\mu_2\text{-Cl})\text{Nd}(\eta^5\text{-C}_9\text{H}_7)_3[\text{Na}(\text{THF})_6]$, each of the C_9H_7^- groups provide three coordination sites and, therefore, the coordination number of each neodymium ion is ten (Figure 1.12).

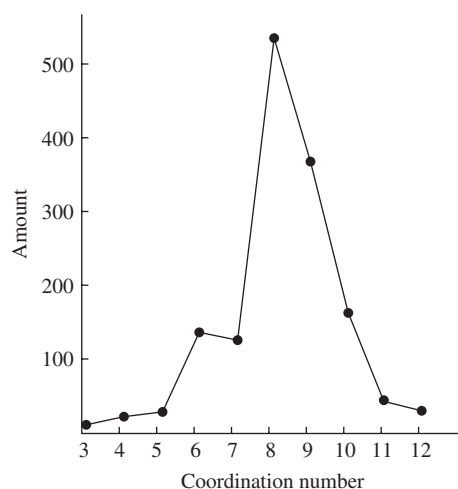
1.4.3.2 Large and Variable Coordination Number

Based on the 1391 complexes that have been structurally characterized and published between 1935 and 1995, we compiled data on the central atoms and their coordination numbers. These results are summarized in Table 1.5 and Figure 1.13. All the coordination numbers are between 3 and 12 and the most common coordination number is eight (37%). Compared with transition metals, lanthanide elements have two distinct characteristics in terms of their coordination number:

1. **Large coordination numbers.** For example, the coordination number of 3d transition metals is generally four or six. However, the most common coordination number of lanthanide complexes is eight or nine. This number is close to the sum of the 6s, 6p, and 5d orbitals. Another fact responsible for the large coordination number of lanthanide complexes

Table 1.5 The statistic number of rare earth complexes with different coordination number [5].

CN ^a	Subtotal	Sc	Y	La	Ce	Pr	Nd	Pm	Sm	Eu	Gd	Tb	Dy	Ho	Er	Tm	Yb	Lu
3	10	2	1		1		1		1	2		1					1	
4	18			3	3				1		1	1					7	2
5	25		4	3	3	3	4				1				3		3	1
6	133	9	19	8	7	12	8		15	10	7		3	1	6	1	20	7
7	121	12	20	10	7	5	10		12	7	6	1	5	1	5	1	13	6
8	534	18	51	31	36	27	53		73	34	24	6	13	16	39	5	68	40
9	367	3	33	31	17	26	61		36	32	25	11	16	12	25	5	21	13
10	160		5	33	20	16	32		18	13	4	1	3	2	2	1	9	1
11	37			14	5	6	4		2	3				1			2	
12	28		1	11	7	2	4			1	1		1					
Sum total	1433	44	134	144	106	97	177		158	102	69	21	41	33	80	13	144	70

^aCN = coordination number.**Figure 1.13** The distribution of rare earth complexes according to coordination number, which were collected from 1391 structurally-characterized coordination complexes reported between 1935 and 1995 [5].

is the large ionic radius of the lanthanide elements. When its coordination number is six, the ionic radius of Fe^{3+} and Co^{3+} are 55 and 54 pm, respectively. However, the ionic radius of La^{3+} , Gd^{3+} , and Lu^{3+} are 103.2, 93.8, and 86.1 pm, respectively.

2. **Variable coordination numbers.** The coordinating stabilization energy (about $4.18 \text{ kJ}\cdot\text{mol}^{-1}$) of lanthanide ions is much smaller than the crystal field stabilization energy of transition metals (typically $\geq 418 \text{ kJ}\cdot\text{mol}^{-1}$). Therefore, the coordinating bonds of lanthanide complexes are not directional and the coordination number varies from 3 to 12.

From Table 1.5 we gather that the number of complexes sorted by their central atoms is 1433. This number is larger than 1391. Two reasons are responsible for this disagreement: (1) the existence of hetero-nuclear lanthanide complexes such as $\{[\text{LaY}(\text{C}_6\text{H}_{11}\text{COO})_4]\text{Cl}_2(\text{CH}_3\text{COCH}_3)_2(\text{H}_2\text{O})_2\}_n$, $\{[\text{ErY}(\text{Gly})_6(\text{H}_2\text{O})_4](\text{ClO}_4)_6(\text{H}_2\text{O})_4\}_n$, and $\{\text{H}[\text{EuLa}_2(\text{DPA})_5(\text{H}_2\text{O})_8](\text{H}_2\text{O})_8\}_n$, and so on, where Gly is glycine and DPA is 2,6-pyridinedicarboxylic acid. (2) In some binuclear or multi-nuclear complexes, the same central ion may have different coordination environments. For example, in the 4,7,13,16,21,24-hexaoxa-1,10-diazabicyclo-(8,8,8)-hexacosane (denoted 222) complex $[(222)(\text{NO}_3)\text{RE}][\text{RE}(\text{NO}_3)_5(\text{H}_2\text{O})]$ ($\text{RE} = \text{Nd}, \text{Sm}$ or Eu), when the central ion is a cation the coordination number is 10 and when the central ion is an anion the coordination number is 11.

1.4.3.3 Coordination Number and Effective Ionic Radius

Recently, by assuming that the distance between different ions is the sum of the ionic radius of the anion and the cation, the distance between anions and cations in thousands of nitrides and oxides have been examined. The influence of coordination number, electron spin, and the geometry of the coordination polyhedron on the ionic radius have also been considered. Under certain conditions, differences in the type of structure will not influence the ionic radius. The crystal cell volume of complexes that have the same anion in a series of analog compounds will be proportional to the cation's radius. Based on the ionic radius proposed by Pauling (O^{2-} , 140 pm; F^- , 133 pm), a suggested set of ionic data was proposed by dividing the distance between different ions using the "Goldschmidt method." This radius was designated the "effective radius." "Effective" implies that these data were deduced from experimental data. The sum of the ionic radii agrees fairly well with the distance between the ions. Table 1.6 lists the effective radii of lanthanide ions for different coordination numbers and at different valence states. For the sake of convenience, some elements that directly bond to lanthanide elements are also listed. These data show that:

1. For the same ion, a larger coordination number leads to a larger effective ionic radius. For example, when the coordination number is 6, 7, 8, 9, 10, and 12 the effective radius of La^{3+} is 103.2, 110, 116.0, 121.6, 127, and 136 pm, respectively.
2. For the same element with the same coordination number, the effective radius will decrease if the valence state increases. For example, when the coordination number is six the effective radius of Ce^{3+} is 101 pm while the effective radius of Ce^{4+} is 87 pm. When the coordination number is eight, the effective radius of Sm^{2+} is 127 pm while that of Sm^{3+} is 102 pm. The reason for this is that one more electron is present in the outer shell for the lower valence ion compared with the higher valence one.
3. When the coordination number and the valence state remain the same, the effective ionic radius will decrease as the atomic number increases. This is caused by lanthanide contraction.

Some ions (for example, H^+ with a coordination number of one or two, C^{4+} with a coordination number of three) show effective radii below zero. This is because they coordinate very tightly to other anions when bonding to them. This strong attraction decreases the distance between the anions and cations even more than the radii of the anions.

Table 1.6 Effective ionic radii of lanthanide ions and other related ions (pm).

Ion	CN ^a	Radii	Ion	CN ^a	Radii	Ion	CN ^a	Radii
La ³⁺	6	103.2	Tb ³⁺	7	98.0	Br ⁻	6	196
	7	110.0		8	104.0	Br ³⁺	4	59
	8	116.0		9	109.5	Br ⁵⁺	3	31
	9	121.6	Tb ⁴⁺	6	76.0	Br ⁷⁺	4	25
	10	127.0		8	88.0		6	39
Ce ³⁺	12	136.0	Dy ²⁺	6	107.0	I ⁻	6	220
	6	101.0		7	113.0	O ²⁻	2	135.0
	7	107.0		8	119.0		3	136.0
	8	114.3	Dy ³⁺	6	91.2		4	138.0
	9	119.6		7	97.0		6	140.0
Ce ⁴⁺	10	125.0		8	102.7		8	142.0
	12	134.0	Ho ³⁺	9	108.3	S ²⁻	6	182.0
	6	87.0		6	90.1	S ⁴⁺	6	34.0
	8	97.0		8	101.5	S ⁶⁺	4	12.0
	10	107.0		9	107.2		6	29.0
Pr ³⁺	12	114.0		10	112.0	Se ²⁻	6	198.0
	6	99.0	Er ³⁺	6	89.0	Se ⁴⁺	6	50.0
	8	112.6		7	94.5	Se ⁶⁺	4	28.0
Pr ⁴⁺	9	117.9		8	100.4		6	42.0
	6	85.0		9	106.2	Te ²⁻	6	221.0
Nd ²⁺	8	96.0	Tm ²⁺	6	103.0	Te ⁴⁺	3	52.0
	8	129.0		7	109.0		4	66.0
Nd ³⁺	9	135.0	Tm ³⁺	6	88.0		6	97.0
	6	98.3		8	99.4	Te ⁶⁺	4	43.0
	8	110.9		9	105.2		6	56.0
Sm ²⁺	9	116.3	Yb ²⁺	6	102.0	N ³⁻	4	146.0
	12	127.0		7	108.0	N ³⁺	6	16.0
	7	122.0		8	114.0	N ⁵⁺	3	-10.4
	8	127.0	Yb ³⁺	6	86.8		6	13.0
Sm ³⁺	9	132.0		7	92.5	P ³⁺	6	44
	6	95.8		8	98.5	P ³⁺	4	17
	7	102.0		9	104.2		5	29
	8	107.9	Lu ³⁺	6	86.1		6	38
Eu ²⁺	9	113.2		8	97.7	As ³⁺	6	58
	12	124.0		9	103.2	As ³⁺	4	33.5
	6	117.0	Sc ³⁺	6	74.5		6	46
	7	120.0		8	87.0	C ⁴⁺	3	-8
Eu ³⁺	8	125.0		6	90.0		4	15
	9	130.0	Y ³⁺	7	96.0		6	16
	10	135.0		8	101.9	Si ⁴⁺	4	26.0
	6	94.7		9	107.5		6	40.0
Gd ³⁺	7	101.0	F ⁻	2	128.5	Ge ²⁺	6	73
	8	106.6		3	130.0	Ge ⁴⁺	4	39
	9	112.0		4	131.0		6	53
	6	93.8		6	133.0	Sn ⁴⁺	4	55
Tb ³⁺	7	100.0	Cl ⁻	6	181.0		5	62
	8	105.3		3	12.0		6	69.0
	9	110.7		4	8.0	H ⁺	1	-38
	6	92.3		6	27		2	-18

^aCN = coordination number.

1.4.4 Tetrad Effect of Lanthanide Elements – Changing Gradation Rules in Lanthanide Coordination Chemistry

Because of gradation filling of electrons into the 4f shell, the properties of many lanthanide compounds show changing gradation with an increase in the atomic number. The lanthanide tetrad effect is an important phenomenon and has also been well studied. Because the separation of lanthanide elements was required before a study of the properties of individual lanthanide elements was possible, the discovery of the lanthanide tetrad effect was related to the separation of lanthanide elements.

It was found that when extracting lanthanide elements with tributyl phosphate at low pH, $\lg D-Z$ showed an “odd–even effect,” which is observed when plotting the logarithm of distribution coefficient D versus the atomic number Z . Straight lines are plotted when Z is odd or even but the odd line is above the even one. Since this report, a lot of data have been reported and presented differently. Figure 1.14 shows typical curves for the change in lanthanide gradation. The lanthanide tetrad effect will also be very clear if the y-axis is not $\lg D$ but $\lg K_{\text{ex}}$

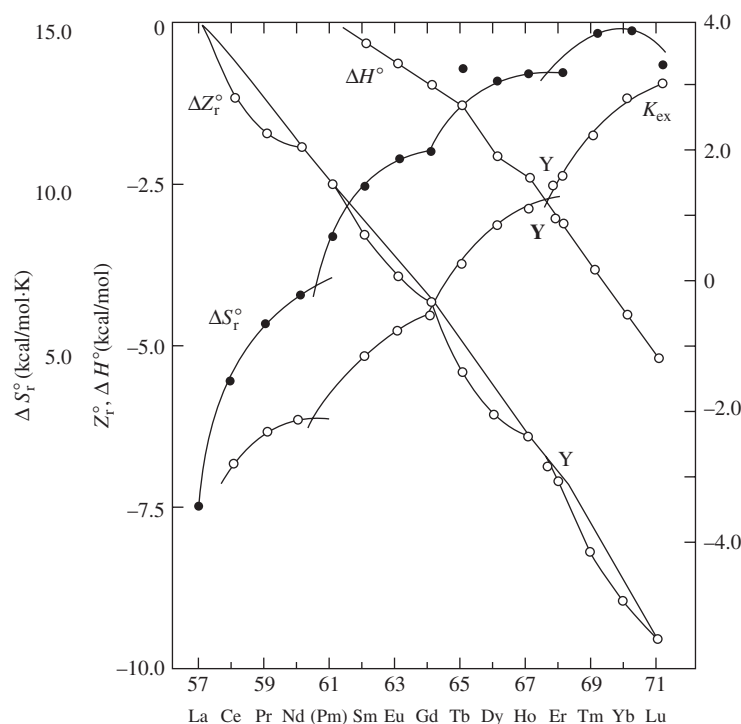


Figure 1.14 The relationship between the atomic number of lanthanides and thermodynamic functions (K_{ex} , ΔH , ΔZ° , and ΔS°) from the extraction system consisting of 2-ethyl hexyl mono(2-ethyl hexyl) ester phosphinate in a dodecane solution [14]. (Reprinted from E.X. Ma, X.M. Yan, S.Y. Wang, *et al.*, “The extraction chemistry of lanthanides with 2-ethyl-hexyle mono (2-ethyl-hexyle) phosphinate oxide,” *Scientia Sinica B: Chemistry* (in Chinese), **5**, 565–573, © 1981, with permission from Science in China Press.)

(extraction equilibrium constant), ΔH (enthalpy variation), ΔZ_r° (free energy variation), and ΔS_r° (entropy variation) of an extraction reaction.

There is a similar phenomenon for trivalent actinide elements. Thus, the tetrad effect is a common characteristic of f-group elements.

Many scientists have shown great interest in the essence of the tetrad effect. Spectral terms and electronic repulsive energies related to constants of the trivalent lanthanide elements are listed in Table 1.7. The ground state spectral terms of lanthanide elements can be sorted into two categories and these are divided by gadolinium: the first category consists of elements before gadolinium, which includes lanthanum, cerium, praseodymium, neodymium and promethium, samarium, europium, and gadolinium, while the second category contains the elements after gadolinium, which includes gadolinium, terbium, dysprosium, holmium, erbium, thulium, ytterbium, and lutetium. As described previously, if one plotted the total orbital angular momentum quantum number L of the ground state versus the atomic number Z the curves will exhibit a tilted W shape as shown in Figure 1.15. Therefore, the tetrad effect can be regarded as a reflection of 4f electronic configuration variations.

To discuss the tetrad effect quantitatively, Nugent analyzed lanthanide and actinide elements using the approximate electronic repulsive energy equation proposed by Jørgensen [15]. He suggested that the electronic repulsive energy H_r between the electrons of the f^q configuration is related to the electron number q . In fact, the macro tetrad effect is a representation of the relationship between H_r and q .

The Jørgensen equation is:

$$H_r = e_0 E^0 + e_1 E^1 + e_2 E^2 + e_3 E^3 \quad (1.3)$$

Table 1.7 Ground state spectral terms and electronic repulsive energy related constants of trivalent lanthanide ions [15].

Trivalent ions	4f electrons	Total angular momentum L	Ground state spectral term	E^1 (eV)	E^3 (eV)	e_1	e_3
La	0	0	1S_0				
Ce	1	3	$^2F_{5/2}$			0	0
Pr	2	5	3H_4	0.56 389	0.0 579	−9/13	−9
Nd	3	6	$^4I_{9/2}$	0.58 758	0.0 602	−27/13	−21
Pm	4	6	5I_4	0.61 019	0.0 652	−54/13	−21
Sm	5	5	$^6H_{5/2}$	0.68 152	0.0 689	−90/13	−9
Eu	6	3	7F_0	0.69 095	0.0 691	−135/13	0
Gd	7	0	$^8S_{7/2}$	0.71 420	0.0 722	−189/13	0
Tb	8	3	7F_6	0.74 655	0.0 755	−135/13	0
Dy	9	5	$^6H_{15/2}$	0.75 872	0.0 756	−90/13	−9
Ho	10	6	5I_8	0.79 851	0.0 774	−54/13	−21
Er	11	6	$^4I_{15/2}$	0.83 934	0.0 802	−27/13	−21
Tm	12	5	3H_6	0.88 552	0.0 836	−9/13	−9
Yb	13	3	$^2F_{7/2}$			0	0
Lu	14	0	1S_0				

(Reprinted from *Journal of Inorganic and Nuclear Chemistry*, **32**, L.J. Nugent, "Theory of the tetrad effect in the lanthanide(III) and actinide(III) series," 3485–3491, 1970, with permission from Elsevier).

where

e_0, e_1, e_2 , and e_3 are all constants obtained from a quantum mechanics calculation
 E^0, E^1, E^2 , and E^3 are obtained from hyperfine emission and absorption spectra

Among them,

$$e_0 = \frac{q(q-1)}{2} \quad (1.4)$$

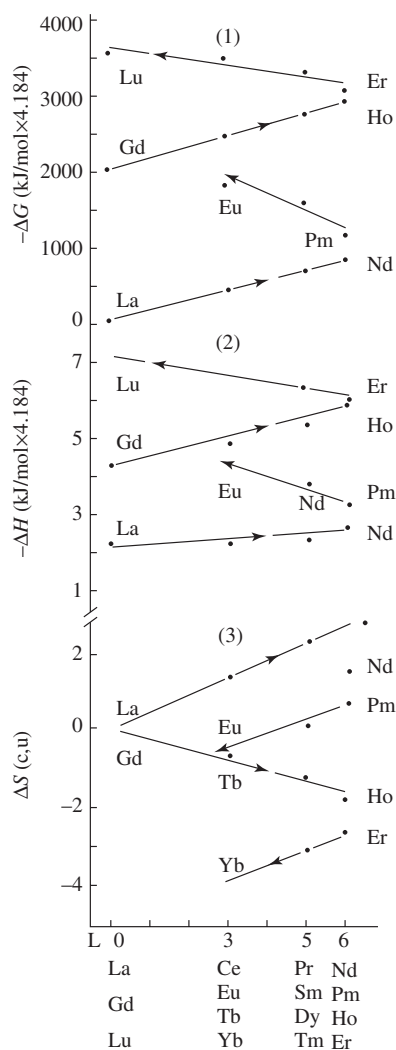


Figure 1.15 The relationship between ΔS , ΔH , ΔG , and L . ΔS , ΔH , and ΔG are thermodynamic constants for the extraction system of N236-xylene/ $\text{RE}(\text{NO}_3)_3$ - HNO_3 . L is the orbital angular momentum quantum number of the lanthanide elements [14]. (Reprinted from E.X. Ma, X.M. Yan, S.Y. Wang, *et al.*, “The extraction chemistry of lanthanides with 2-ethyl-hexyle mono (2-ethyl-hexyle) phosphinate oxide,” *Scientia Sinica B: Chemistry* (in Chinese), **5**, 565–573, © 1981, with permission from Science in China Press.)

The first term of H_r increases regularly as q increases. Therefore, it does not contribute to a periodic change in H_r . The term $e_2 E^2$ can be ignored because all functions related to this term approach zero in the ground state. Additionally,

$$e_1 = 9/8\{ | < S(S-1) > | - S(S+1) \} \quad (1.5)$$

where

$< S(S+1) >$ is the weighting of a spectral term with a total spin quantum number S
 l is the angular quantum number

and

$$< S(S+1) > = \frac{3}{4}q \left[1 - \frac{(q-1)}{4l+1} \right] \quad (1.6)$$

for f electrons $l=3$, and thus

$$< S(S+1) > = \frac{3}{4}q \left[1 - \frac{(q-1)}{13} \right] \quad (1.7)$$

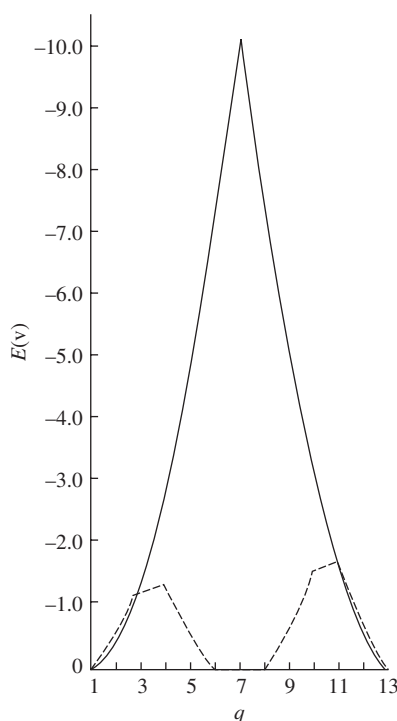


Figure 1.16 The ground state electronic repulsive stabilization energy E as a function of the 4f electron number q (the contribution from the E^1 term in Equation 1.3, solid line; the contribution from the E^3 term in Equation 1.3, dashed line) [15]. (Reprinted from *Journal of Inorganic and Nuclear Chemistry*, **32**, L.J. Nugent, "Theory of the tetrad effect in the lanthanide(III) and actinide(III) series," 3485–3491, 1970, with permission from Elsevier.)

From Table 1.7 we can see that e_1 changes with the 4f electron number q . e_1 reaches a maximum when $q = 7$. By plotting $e_1 E$ versus q we get Figure 1.16. The solid line in Figure 1.16 reaches a maximum at f^7 (Gd^{3+}). This is an obvious reflection of the half-full effect of its 4f orbital. It is generally referred as the “gadolinium broken effect.”

It can be seen from Table 1.7 that although E^3 increases regularly as q increases, e_3 changes periodically. The dashed line in Figure 1.16 shows the plot of $e_3 E^3$ versus q . Two maxima are observed at f^{3-4} (Nd^{3+} – Pm^{3+}) and f^{10-11} (Ho^{3+} – Er^{3+}), respectively. This result implies that three steady states are present at f^7 , f^{3-4} , and f^{10-11} , respectively. This explains the tetrad effect because the three intersections in the tetrad effect are in the same position. However, the two maxima at f^{3-4} and f^{10-11} are six times smaller than the one at f^7 . It is very difficult to observe such small stabilization energies in chemical reactions. This explains why the tetrad effect was discovered so much later than the gadolinium broken effect.

It should be pointed out that not all the ions discussed here are affected by the outer fields. In fact, lanthanide ions may be affected by solvents or coordination fields in chemical reactions. For example, E^1 and E^3 will change because of the coordination effect of water or organic molecules in an extraction. In addition, the amount of change would be different in different media. The tetrad effect would thus be different in different systems. The tetrad effect not only relates to the electronic configurations of lanthanide elements but is also affected by the surrounding conditions. Currently it is still not possible to predict the tetrad effect or to calculate it quantitatively. Tetrad effect theory still needs to be improved and further data need to be accumulated.

1.5 Coordination Chemistry of Inorganic Compounds

1.5.1 Rare Earth Hydroxides

Under general conditions, rare earth hydroxides $\text{RE}(\text{OH})_3 \cdot n\text{H}_2\text{O}$ precipitate from a high pH solution as a gel. However, they are unstable during heating and usually lose water to become $\text{REO}(\text{OH})$ or RE_2O_3 when the temperature approaches or exceeds 200 °C. From lanthanum to lutetium, the dehydration temperature decreases with an increase in atomic number because of a decrease in the ionic ratio.

Single crystals of rare earth hydroxides can be obtained by a hydrothermal method. At 190–420 °C and from 1.2×10^6 to 7×10^7 Pa, rare earth hydroxides can be grown from RE_2O_3 – H_2O – NaOH systems after prolonged treatment.

Structure: $\text{Lu}(\text{OH})_3$ and $\text{Sc}(\text{OH})_3$ have a cubic system but all the other rare earth single crystals have hexagonal systems. In the hexagonal system, two $\text{RE}(\text{OH})_3$ units are present in each cell. As a μ_3 -bridge, each hydroxide group links three rare earth ions and there are thus nine oxygen atoms around each RE^{3+} ion and their coordination number is nine. No hydrogen bonds exist in the cells as all three lone pair electrons of the oxygen atoms are occupied by rare earth ions and form a tri-capped tri-angular prism polyhedron. In cubic systems, there are eight $\text{RE}(\text{OH})_3$ units in each cell. As a μ_2 -bridge, each hydroxide group links two rare earth ions and the rare earth ions are six coordinated by six oxygen atoms and form an octa-polyhedron. In this infinite network, strong hydrogen bonds exist between the hydroxide groups (Figure 1.17).

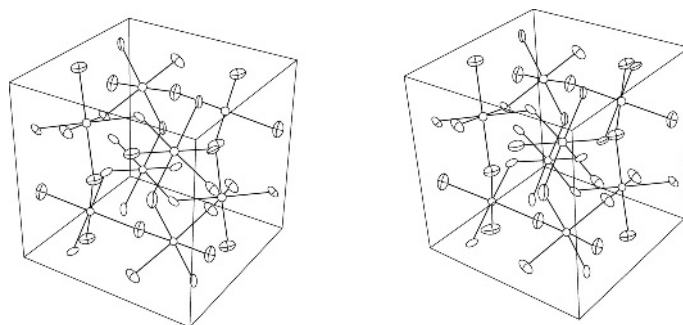


Figure 1.17 Crystal structures of $\text{Lu}(\text{OH})_3$ [16]. (Reprinted from *Journal of Inorganic and Nuclear Chemistry*, **42**, D.F. Mullica, and W.O. Milligan, "Structural refinement of cubic $\text{Lu}(\text{OH})_3$," 223–227, 1980, with permission from Elsevier.)

1.5.2 Rare Earth Halide and Perchlorate Compounds

Rare earth halide compounds easily absorb water from their surroundings to form hydrates, $\text{RECl}_3 \cdot n\text{H}_2\text{O}$. For lanthanum, cerium, praseodymium, $n = 7$, while for neodymium to lutetium and scandium, yttrium, $n = 6$. Non-hydrated rare earth halides can be directly obtained by the reaction of rare earth metals with corresponding halide gases or by substitution reactions of rare earth metals with halide mercury. They can not, however, be obtained by heating the hydrated halide because the hydrate will hydrolyze to form REOX , where X represents the corresponding halide. Another commonly used method is to mix $\text{REX}_3 \cdot n\text{H}_2\text{O}$ and excess NH_4X ($\text{RECl}_3/\text{NH}_4\text{Cl} = 6$, $\text{REI}_3/\text{NH}_4\text{I} = 12$) into a solution and slowly heat under vacuum to remove all the water, upon which heating is slowly continued up to 300°C and until all the ammonium halide is entirely sublimated.

The solubility of rare earth fluorides REF_3 is very low, the $\text{p}K_{\text{sp}}$ ranges from 19 to 15 for lighter rare earth lanthanum, cerium, praseodymium, and neodymium to heavier rare earth ytterbium and lutetium, respectively.

Structure: Non-hydrated rare earth fluorides have two different crystal systems, a hexagonal system (lanthanum to terbium) and an orthorhombic system (dysprosium to lutetium, yttrium). In the crystal of LaF_3 , the central ion is nine coordinated by nine fluoride atoms. Each fluoride atom further connects with two lanthanum atoms through a μ_3 -bridge to form an infinite polymer.

Hydrates of rare earth chlorides also have two different crystal systems: a triclinic system for lanthanum, cerium, and praseodymium, as well as a monoclinic system for neodymium to lutetium and yttrium. $\text{CeCl}_3 \cdot 7\text{H}_2\text{O}$, as an example of the former system, is different from the above infinite polymer as two cerium atoms are connected by two μ_2 -bridges to form a dimer. The formula for this dimer is $[(\text{H}_2\text{O})_7\text{Ce}(\mu_2\text{-Cl})_2\text{Ce}(\text{H}_2\text{O})_7]\text{Cl}_4$ as shown in Figure 1.18. Therefore, the coordination number of cerium is nine and the polyhedron takes on a destroyed mono-capped square antiprism configuration.

$\text{GdCl}_3 \cdot 6\text{H}_2\text{O}$ exists as a single molecule and can be represented as $[\text{GdCl}_2 \cdot 6\text{H}_2\text{O}] \cdot \text{Cl}$. The coordination number of gadolinium is eight and the uncoordinated chloride is present in the lattice because it forms six hydrogen bonds with coordinated water molecules.

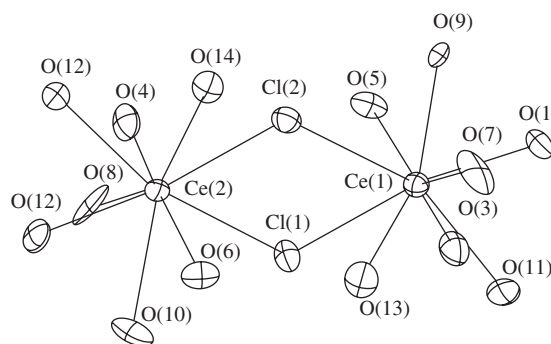


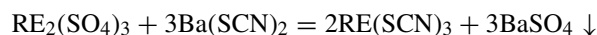
Figure 1.18 Structure of the $[(\text{H}_2\text{O})_7\text{Ce}(\mu_2\text{-Cl})_2\text{Ce}(\text{H}_2\text{O})_7]^{4+}$ in hydrated cerium chloride [17]. (Reprinted from E.J. Peterson, E.I. Onstott, and R.B.V. Dreele, "A refinement of cerium(III) trichloride heptahydrate in space group $P1$," *Acta Crystallographica*, **B35**, no. 4, 805–809, 1979, with permission from International Union of Crystallography.)

Because its ionic potential Z/R is relative small, the coordination capability of the perchlorate group to rare earth ions is relatively weak compared with other oxygen containing acid groups. For example, in $\text{RE}(\text{ClO}_4)_3 \cdot 6\text{H}_2\text{O}$ the central ion is coordinated to water molecules and all the perchlorate anions only exist in the lattice and are not connected to the rare earth central ion. However, it does coordinate to rare earth ions by adopting mono- or bidentate modes depending on the coordination capability of the competitive ligands. For example, in the complex $[\text{Nd}(\text{ClO}_4)_2(\text{ph}_3\text{PO})_4]\text{ClO}_4 \cdot \text{C}_2\text{H}_5\text{OH}$, two perchlorate groups adopt a bidentate mode to coordinate to the neodymium ion, while the third one exists in the lattice (Figure 1.19).

1.5.3 Rare Earth Cyanide and Thiocyanate Compounds

Rare earth cyanide compounds can be obtained by a reaction between the corresponding metal and cyanic acid in liquid ammonia, but when rare earth metals react with cyanic acid directly under ambient conditions the related cyanide compounds can not be obtained, but the products will be rare earth nitride and carbide.

The non-hydrated rare earth thiocyanate can be obtained by a reaction between the corresponding metal and NH_4SCN in liquid ammonia or by the dehydration of the corresponding hydrated thiocyanate at 1333 Pa and 50 °C. However, the hydrated thiocyanate can be prepared by the following double replacement reactions:



or



Structures: In rare earth cyanides the rare earth ions prefer to coordinate to carbon and not nitrogen because of the negative charge of the cyanide cation that is present at the carbon side

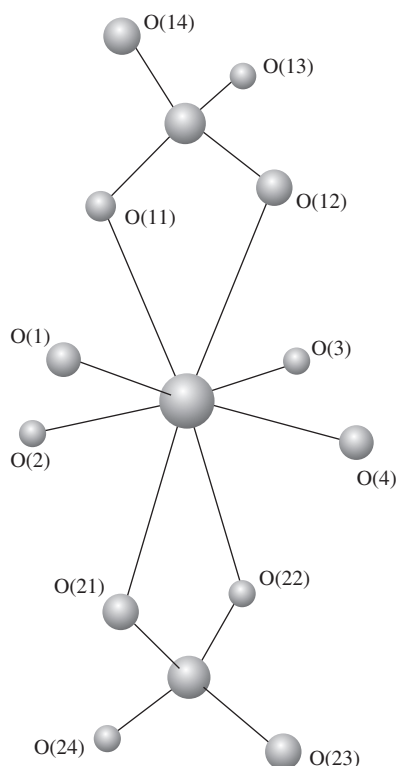


Figure 1.19 The cation structure in the complex $[\text{Nd}(\text{ClO}_4)_2(\text{ph}_3\text{PO})_4]\text{ClO}_4 \cdot \text{C}_2\text{H}_5\text{OH}$ [18].

[19] (Figure 1.20). On the other hand, when rare earth thiocyanates are the ligands, the rare earth ions prefer to coordinate to the nitrogen and not the sulfur (Figure 1.21).

1.5.4 Rare Earth Carbonate Compounds

The solubility of rare earth carbonates is fairly low and ranges from 10^{-5} to 10^{-6} mol L^{-1} . Rare earth carbonates can be obtained by the addition of ammonium carbonate to a solution of a rare earth water-soluble salt. In this case, the precipitates will all be hydrates. Lanthanum to neodymium carbonates contain eight water molecules while neodymium to lutetium carbonates contain two water molecules only. Rare earth carbonates can be dissolved in alkali metal carbonate solutions and form a double salt of alkali metals.

Structure: The coordination modes of carbonates are fairly abundant and they can be monodentate, bidentate, or multidentate when coordinated to the central ion (Figure 1.22). For instance, in the crystal of $\text{La}_2(\text{CO}_3)_3 \cdot 8\text{H}_2\text{O}$ the carbonate groups have modes a, b, and c as shown in Figure 1.22 when coordinated to the lanthanum ion. In the $\text{Nd}(\text{OH})\text{CO}_3$ crystal, the carbonate groups have the d mode when coordinating to neodymium ions. In this compound, the coordination number of neodymium ion is nine. A layer-like polymer is formed by hydroxyl linkages and a carbonate bridge. The $\text{Y}(\text{OH})\text{CO}_3$ crystal belongs to the orthorhombic system

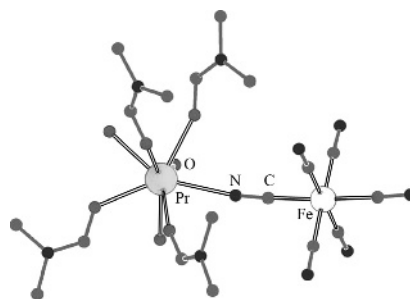


Figure 1.20 A projection of the bi-nuclear unit of $[\text{Pr}(\text{dmf})_4\text{Fe}(\text{CN})_6(\text{H}_2\text{O})_4]$. Lattice water molecules have been omitted for clarity [19a] (Reprinted from *Coordination Chemistry Review*, **250**, S. Tanase and J. Reedijk, “Chemistry and magnetism of cyanido-bridged d-f assemblies,” 2501–2510, 2006, with permission from Elsevier.)

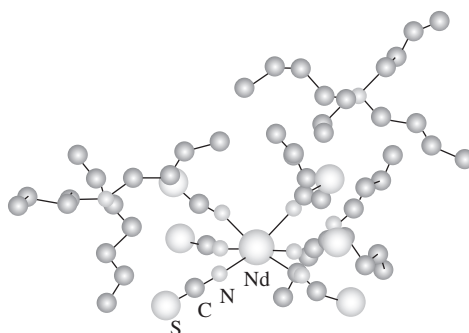


Figure 1.21 The structure of the complex $[(\text{C}_4\text{H}_9)_4\text{N}]_3\text{Nd}(\text{NCS})_6$ [20].

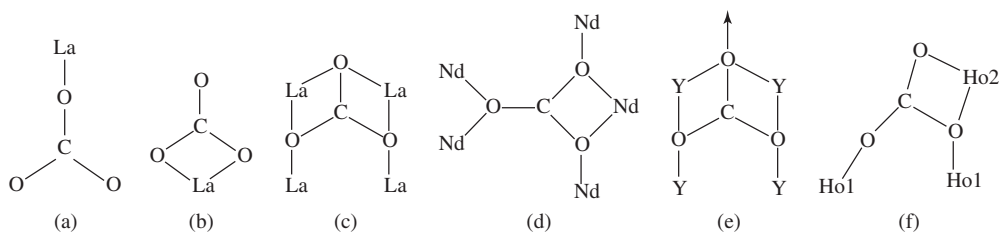


Figure 1.22 Six coordination modes for different rare earth carbonates.

and the coordination number of yttrium is nine (Figure 1.23). Two coordination places are taken up by hydroxyls through a μ_2 -bridge and the other seven are taken up by one carbonate group each (see Figure 1.22e) to form a polymer. Under thermo-hydration (250–300 °C) conditions, the heavier rare earth carbonates will end up as $\text{RE}_2(\text{OH})_4\text{CO}_3$, where RE = yttrium, holmium, erbium, thulium, or ytterbium. In the crystal of $\text{Ho}_2(\text{OH})_4\text{CO}_3$ (Figure 1.22f), holmium ions have two different coordination numbers: Ho1 ions have seven while Ho2 ions have eight, and the hydroxyls adopt μ_2 and μ_3 coordination modes to connect to the holmium ions.

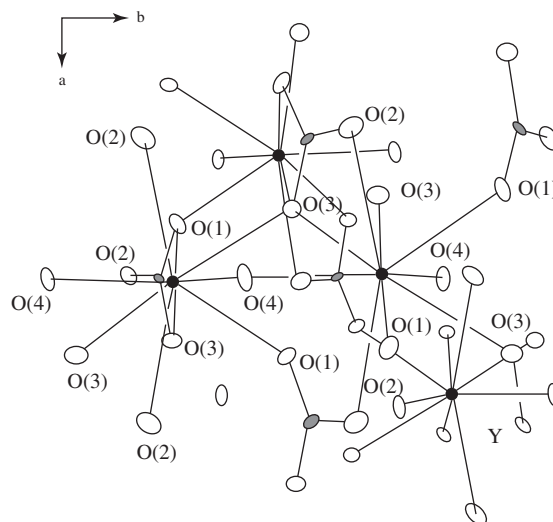


Figure 1.23 The structure of Y(OH)CO_3 [21]. (Reprinted from G.W. Beall, W.O. Milligan, and S. Mroczkowski, "Yttrium carbonate hydroxide," *Acta Crystallographica*, **B32**, no. 11, 3143–3144, 1976, with permission from International Union of Crystallography.)

1.5.5 Rare Earth Oxalate Compounds

Oxalic acid is a precipitation agent for rare earth ions. The solubility of rare earth oxalates range from 10^{-3} to 10^{-4} mol L^{-1} in neutral solutions. The precipitate usually contains coordinated and/or lattice water molecules, $\text{RE}_2(\text{C}_2\text{O}_4)_3 \cdot n \text{H}_2\text{O}$, where $n = 10$ for lanthanum to erbium and yttrium while $n = 6$ for holmium, erbium, thulium, ytterbium to lutetium and scandium.

Structure: In the $\text{Nd}_2(\text{C}_2\text{O}_4)_3 \cdot 10\text{H}_2\text{O}$ molecule, the central neodymium ion is nine coordinated by nine oxygen atoms of which six are contributed by the three oxalic groups and the other three come from water molecules. The coordinated polyhedron can be described as a destroyed tri-capped triangular prism. In this molecule, each oxalic group is bidentate coordinated from both sides and acts as a bridge to connect two neodymium ions. Therefore, the molecular formula is represented by $\{[\text{Nd}_2(\text{C}_2\text{O}_4)_3 \cdot 6\text{H}_2\text{O}] \cdot 4\text{H}_2\text{O}\}_n$ (Figure 1.24).

In alkali metal salt solutions, the solubility of rare earth oxalates is higher compared with that in water and this is due to the formation of a double salt. Depending on their formation conditions, they exist in different forms. At least three of these forms have been structurally characterized: $\text{NH}_4\text{RE}(\text{C}_2\text{O}_4)_2 \cdot n\text{H}_2\text{O}$, where $n = 3$ for lanthanum to neodymium, $n = 1$ for samarium to thulium; $\text{K}_3\text{RE}(\text{C}_2\text{O}_4)_3 \cdot n\text{H}_2\text{O}$ and $\text{K}_8\text{RE}_2(\text{C}_2\text{O}_4)_7 \cdot 14\text{H}_2\text{O}$ for the latter, $\text{RE} =$ terbium, dysprosium, erbium, ytterbium, and yttrium are analogs. The structure of the anion in $\text{K}_8[\text{RE}_2(\text{C}_2\text{O}_4)_7] \cdot 14\text{H}_2\text{O}$ is represented in Figure 1.25. It is worth noting that in this anion two different coordination modes are present for the oxalate group. One is a bidentate coordination from both sides of the oxalate group and the other is coordination by the bidentate ligand from one side only.

Among these, a is the most common mode, as in the complex $\{[(\text{CH}_3)_3\text{NC}_{16}\text{H}_{33}]_3\text{Nd}(\text{NO}_3)_6\}_2$. Nitrate groups take on modes a and c when coordinated to neodymium ions. However, in the compound $[(\text{C}_4\text{H}_9)_4\text{N}]_3\text{Nd}(\text{NO}_3)_6$ the nitrate group only adopts mode a (Figure 1.27).

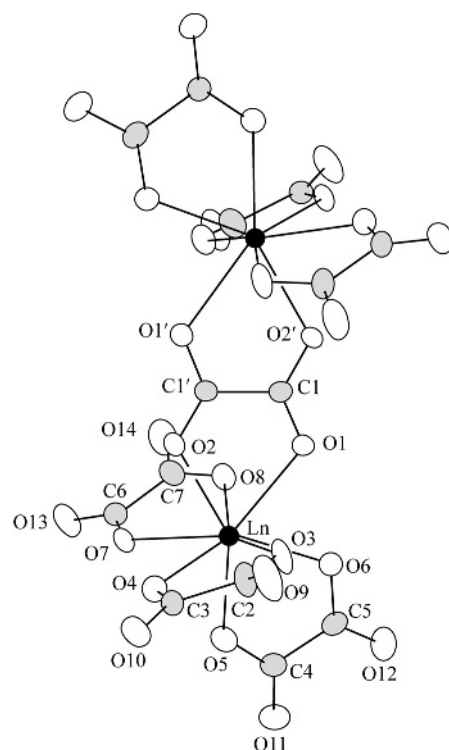


Figure 1.25 The anion structure in the complex $K_8RE_2(C_2O_4)_7 \cdot 14H_2O$ [23]. (Reprinted from *Inorganica Chimica Acta*, **82**, no. 2, I.A. Kahwa, F.R. Fronczek, and J. Selbin, "The crystal and molecular structures of potassium- μ -oxalato-di [tris-oxalato-lanthanate(III)]-14-hydrates $K_8[Ox_3LnOxLnOx_3]14H_2O$ [$Ln = Tb, Dy, Er, Yb, Y$]," 167–172, 1984, with permission from Elsevier.)

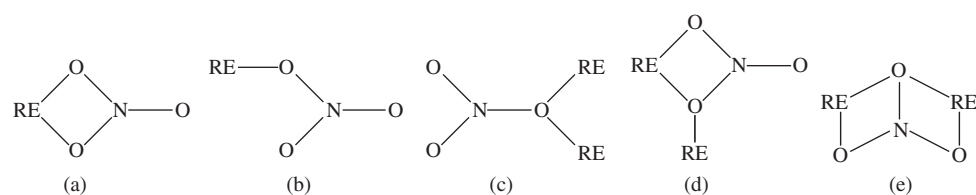


Figure 1.26 Five coordination modes in different rare earth compounds.

1.5.7 Rare Earth Phosphate Compounds

The solubility of rare earth phosphates is fairly low in neutral or acidic aqueous solutions, for example, the K_{sp} values for $LaPO_4$ and $CePO_4$ are 4.0×10^{-23} and 1.6×10^{-23} , respectively. Therefore, rare earth phosphates can be obtained by the reaction of soluble rare earth salts with alkali metal phosphates. Usually, the product has the following formula: $REPO_4 \cdot nH_2O$

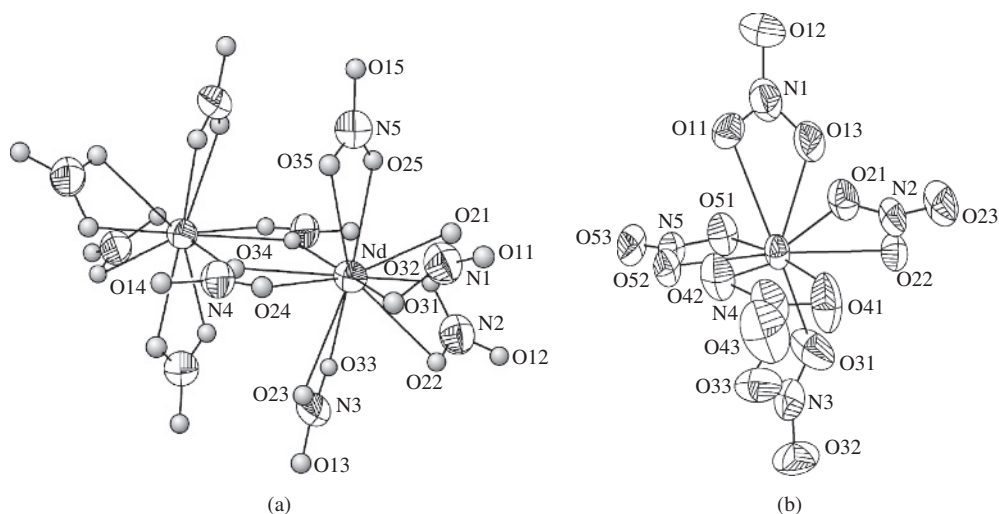


Figure 1.27 Anion structures in the complexes $\{[(\text{CH}_3)_3\text{NC}_{16}\text{H}_{33}]_3\text{Nd}(\text{NO}_3)_6\}_2$ (a) and $[(\text{C}_4\text{H}_9)_4\text{N}]_3\text{Nd}(\text{NO}_3)_6$ (b) [24].

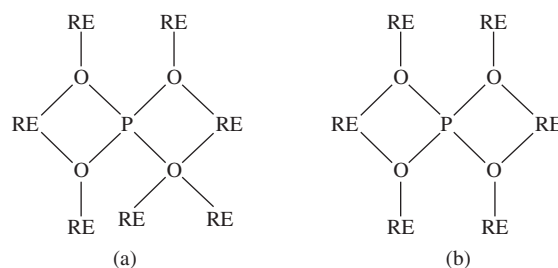


Figure 1.28 Two coordination modes for REPO_4 .

where $n = 0.5\text{--}4$. Single crystals of these phosphates may be obtained by melting them at high temperatures using lead pyro-phosphate as a medium.

Structure: These compounds can be divided into two groups according to structure.

For the lighter rare earth elements (lanthanum to gadolinium), REPO_4 belongs to the monoclinic system. The coordination number of the central ions is nine. All nine oxygen atoms are contributed by the phosphate groups. The coordination modes of the phosphate group is shown in Figure 1.28a. The coordination polyhedron has a destroyed pentagonal di-pyramid configuration. Five oxygen atoms form an equatorial plane with a rare earth ion in the center and two phosphate groups capped on the top and bottom of the equatorial plane. The coordination status of the central ion and the crystal structure of the REPO_4 compounds are shown in Figure 1.29.

The REPO_4 structure for the heavier rare earth elements (terbium to lutetium, yttrium, and scandium) belong to the tetragonal system. The coordination number of the central ions is

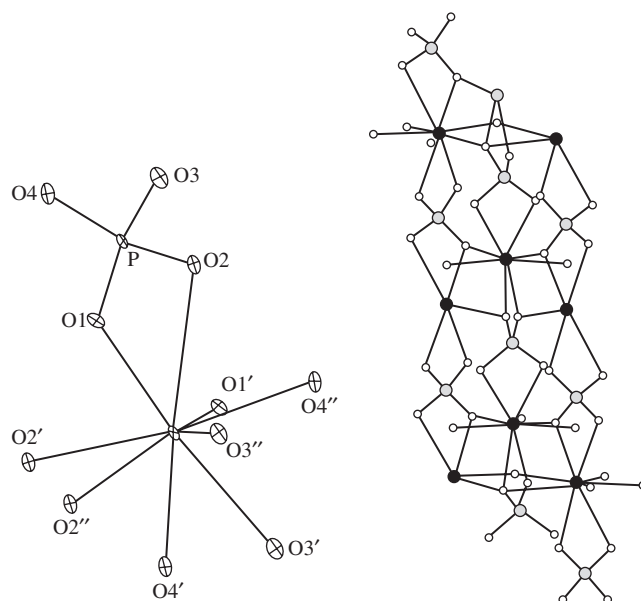


Figure 1.29 The coordination status of the central ion and the crystal structure of the REPO_4 (RE = lanthanum to gadolinium) compounds [25]. (Reprinted from *Inorganica Chimica Acta*, **109**, no. 2, D.F. Mullica, D.A. Gossie, and L.A. Boatner, "Coordination geometry and structural determinations of SmPO_4 , EuPO_4 and GdPO_4 ," 105–110, 1985, with permission from Elsevier.)

eight and they are filled by the phosphate, which forms a three-dimensional polymer. The coordination mode of the phosphate group is shown in Figure 1.28b.

1.5.8 Rare Earth Sulfate Compounds

When rare earth oxides, hydroxides, or carbonates react with dilute sulfuric acid, rare earth sulfate hydrates are obtained and they have the formula $\text{RE}_2(\text{SO}_4)_3 \cdot n\text{H}_2\text{O}$ where $n = 3, 4, 5, 6, 8$, and 9. The most common is $n = 9$ for lanthanum and cerium and $n = 8$ for praseodymium to lutetium and yttrium. Anhydrous compounds may be obtained by heating the respective rare earth sulfate hydrate at 155–260 °C, however, they easily absorb water to become hydrated again.

Structure: The $\text{La}_2(\text{SO}_4)_3 \cdot 9\text{H}_2\text{O}$ structure consists of an infinite network. In this molecule, lanthanum ions have two coordination environments (La1 and La2 in Figure 1.30a). La1 is coordinated to 12 oxygen atoms from six bidentate sulfate groups, while for La2 the coordination number is nine and consists of six oxygen atoms that are contributed from six water molecules and the other three are occupied by three monohapto sulfate groups. The coordination polyhedron has a tri-capped triangular prism configuration. The rest of the water molecules exist in the network through hydrogen bonds connected to oxygen atoms. Therefore, the formula may be represented as $\{[\text{La}_2(\text{SO}_4)_3 \cdot 6\text{H}_2\text{O}] \cdot 3\text{H}_2\text{O}\}_n$.

$\text{Pr}_2(\text{SO}_4)_3 \cdot 8\text{H}_2\text{O}$ is also an infinite network. In this molecule, the coordination number of praseodymium is eight, among which four of the oxygen atoms come from four water molecules

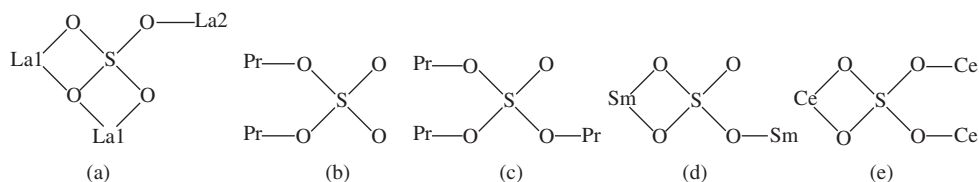


Figure 1.30 Five coordination modes of the sulfate group in different rare earth compounds.

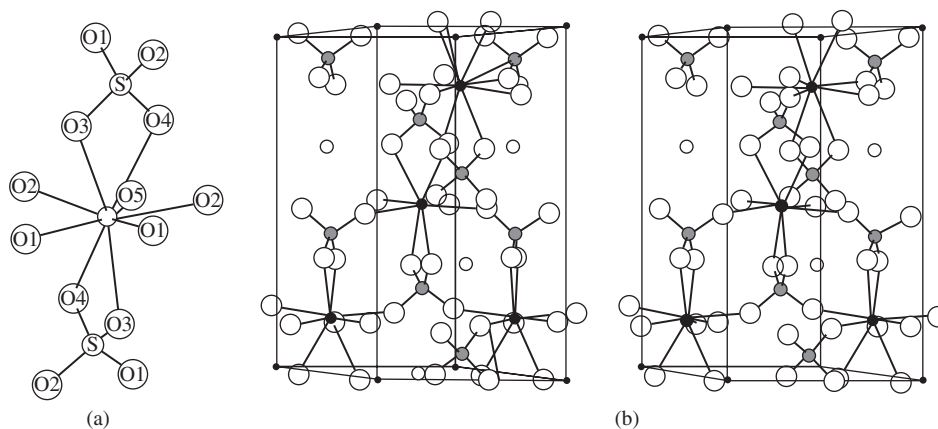


Figure 1.31 (a) The coordination status of the central cerium ion in $\text{NaCe}(\text{SO}_4)_2 \cdot \text{H}_2\text{O}$; (b) the crystal structure of $\text{NaCe}(\text{SO}_4)_2 \cdot \text{H}_2\text{O}$ [26]. (Reprinted from O. Lindgren, "The crystal structure of sodium cerium(III) sulfate hydrate, $\text{NaCe}(\text{SO}_4)_2 \cdot \text{H}_2\text{O}$, *Acta Chemica Scandinavica*, **A31**, 591–594, 1977, with permission from Forlagsforeningen Acta Chemica Scandinavica.)

and the rest come from four monohapto sulfate groups. The coordination polyhedron takes on a square antiprism configuration. In this molecule, the sulfate groups adopt two different coordination modes to coordinate to the central ions and they are present as bidentate (Figure 1.30b) and tridentate bridges (Figure 1.30c).

Rare earth double salts can be formed by the reaction of rare earth sulfates with a corresponding alkali or alkaline earth sulfate. For the former, the general formula is $\text{RE}_2(\text{SO}_4)_3 \cdot \text{M}_2\text{SO}_4 \cdot n\text{H}_2\text{O}$, where $n = 0, 2$ or 8 . $\text{NH}_4\text{Sm}(\text{SO}_4)_2 \cdot 4\text{H}_2\text{O}$ has an infinite chain-like configuration. In this molecule, samarium is coordinated to nine oxygen atoms, where three of them come from three water molecules and the rest come from two bidentate sulfate groups and two monohapto sulfate groups. The sulfate groups adopt a bridging coordination mode as shown in Figure 1.30d. The molecular formula should thus be $\{\text{NH}_4[\text{Sm}(\text{SO}_4)_2 \cdot 3\text{H}_2\text{O}] \cdot \text{H}_2\text{O}\}_n$.

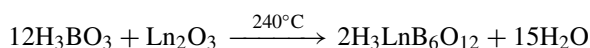
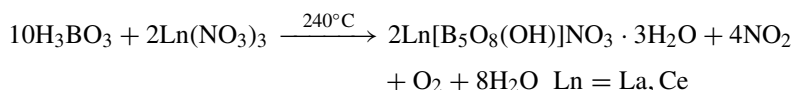
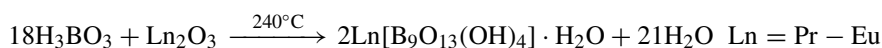
The crystal structure of $\text{NaCe}(\text{SO}_4)_2 \cdot \text{H}_2\text{O}$ has a trigonal system and the central cerium ion is coordinated to nine oxygen atoms. The oxygen atoms, four from monohapto sulfate groups and one from a water molecule form an equatorial plane, and each bidentate sulfate group cap the top and bottom positions of the equatorial plane (Figure 1.31a). Sodium ions are coordinated to six oxygen atoms from the sulfate groups and they bridge between the cerium ions to form an infinite network (Figure 1.31b).

1.5.9 Rare Earth Borate Compounds

Many borate structures exist and are fairly interesting. They are stable in air and have been considered for use as important nonlinear optical materials and as hosts for luminescent materials, particularly when the excitation of high energy photons is required, for example, $\text{LuMgB}_5\text{O}_{11}$: Tb, Ce and SrB_4O_7 : Eu.

In the borates, the boron atoms are coordinated to oxygen atoms forming either a tetrahedral or a triangular configuration. $[\text{BO}_4]$ or $[\text{BO}_3]$ units can exist individually in the borate. However, it is more common for them to form a one-dimensional chain, two-dimensional plane, or three-dimensional network by sharing corners and by sharing edges in a few instances.

In 2001 Lin and coworkers found that in a sealed reaction system containing melted boric acid and trivalent rare earth cations, a series of new rare earth polyborates were obtained. The structure of these resulting products was found to be highly dependent on reaction conditions, such as the starting materials used, the temperature, the water content, the ratio of RE/B, and the radius of the rare earth ions. The lighter rare earth elements, lanthanum, cerium, praseodymium or neodymium, prefer to form $\text{Ln}[\text{B}_5\text{O}_8(\text{OH})_2]$ or $\text{Ln}[\text{B}_8\text{O}_{11}(\text{OH})_5]$. When the radius is contracted further $\text{Ln}[\text{B}_6\text{O}_9(\text{OH})_3]$ ($\text{Ln} = \text{Sm} - \text{Lu}$) is formed. These formation reactions can be summarized as follows:



As representative examples the $[\text{LnB}_6\text{O}_{11}]$ layer in $\text{Ln}[\text{B}_8\text{O}_{11}(\text{OH})_5]$ or $\text{Ln}[\text{B}_9\text{O}_{13}(\text{OH})_4] \cdot \text{H}_2\text{O}$, and the $[\text{LnB}_5\text{O}_9]$ layer in $\text{Ce}[\text{B}_5\text{O}_8(\text{OH})]\text{NO}_3 \cdot 3\text{H}_2\text{O}$ are presented in Figure 1.32. The fundamental building blocks of (a) $\text{Ln}[\text{B}_8\text{O}_{11}(\text{OH})_5]$, (b) $\text{Ln}[\text{B}_9\text{O}_{13}(\text{OH})_4] \cdot \text{H}_2\text{O}$, and (c) $\text{Ce}[\text{B}_5\text{O}_8(\text{OH})]\text{NO}_3 \cdot 3\text{H}_2\text{O}$ are shown in Figure 1.33.

1.6 Outlook

The unique properties of rare earth elements, for instance, the hard Lewis acid character, the sharp, wide-range (from near IR to UV) long-lived luminescence, and the high magnetic moment with long electron-spin relaxation time, etc. and the potential applications of their complexes, are the main driving forces for the development of the coordination chemistry of rare earth. In this chapter, fundamental rules for rare earth complexes and the coordination chemistry of rare earth with some simple but important ligands are briefly discussed. At present, some of these aspects are still not clear enough. There is no doubt that the inherent properties of these complexes will be understood more quantitatively as research tools and technologies are improved.

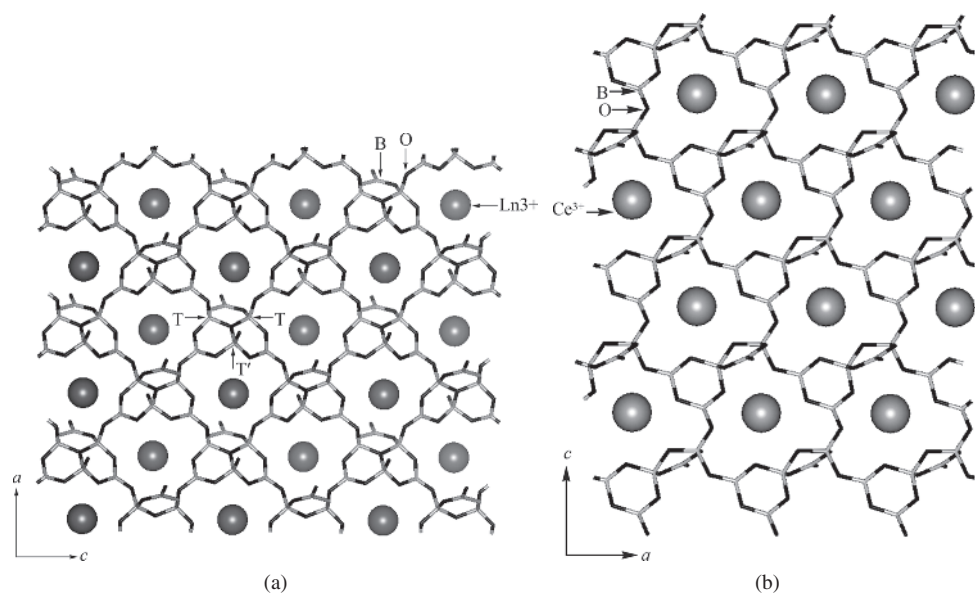


Figure 1.32 (a) The $[\text{LnB}_6\text{O}_{11}]$ layer in $\text{Ln}[\text{B}_8\text{O}_{11}(\text{OH})_5]$ and $\text{Ln}[\text{B}_9\text{O}_{13}(\text{OH})_4]\cdot\text{H}_2\text{O}$; (b) the $[\text{LnB}_5\text{O}_9]$ layer in $\text{Ce}[\text{B}_5\text{O}_8(\text{OH})]\text{NO}_3\cdot 3\text{H}_2\text{O}$. The borate network is displayed in stick style and the balls represent the rare earth cations [27]. (Reprinted with permission from J.H. Lin, Y.X. Wang, L.Y. Li, *et al.*, "Rare earth borates: an overview from the structural chemistry viewpoint," in G. Meyer, D. Naumann and L. Wesemann (eds.), *Inorganic Chemistry in Focus II*, 293–378 (Figure 16.21). © Wiley-VCH Verlag GmbH & Co. KGaA, Weinheim. © 2005.)

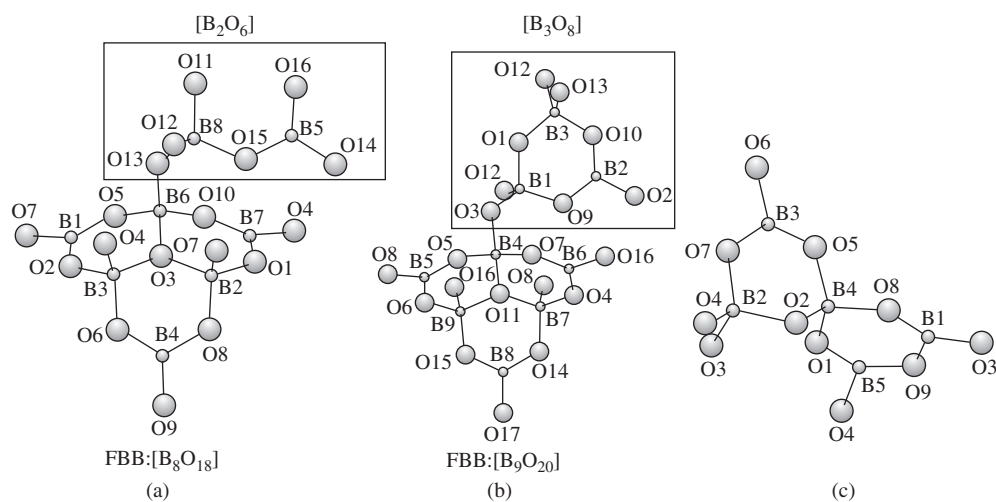


Figure 1.33 The fundamental building block of: (a) $\text{Ln}[\text{B}_8\text{O}_{11}(\text{OH})_5]$; (b) $\text{Ln}[\text{B}_9\text{O}_{13}(\text{OH})_4]\cdot\text{H}_2\text{O}$; and (c) $\text{Ce}[\text{B}_5\text{O}_8(\text{OH})]\text{NO}_3\cdot 3\text{H}_2\text{O}$ [28]. (Reprinted with permission from L.Y. Li, X.L. Jin, G.B. Li, *et al.*, "Novel rare earth polyborates. 2. Syntheses and structures," *Chemistry of Materials*, **15**, 2253–2260, 2003. © 2003 American Chemical Society.)

Acknowledgments

We thank the National Basic Research Program (**2006CB601103**) and the NNSFC (**50772003**, **20821091**, **20971006**, **90922004**) for their financial support.

References

- [1] Xu, G., Huang, C., and Gao, S. (1995) *The Chemistry of Rare Earth Elements, Rare Earths (in Chinese)*, Vol. **I**, 2nd edn, Ch 2 (ed. G. Xu), Metallurgical Industry Press, Beijing.
- [2] Goldschmidt, Z.B. (1978) *Atomic Properties (Free Atom), Handbook on the Physics and Chemistry of Rare Earths*, Vol. **I**, 2nd edn, Ch 1 (eds K.A. Gschneidner and L. Eyring), North Holland Publishing Company, Amsterdam, pp. 1–171.
- [3] Cotton, S. (2006) *Lanthanide and Actinide Chemistry*, John Wiley & Sons, Ltd, Chichester.
- [4] Xu, G. and Wang, X. (1987) *The Structure of Matters (in Chinese)*, 2nd edn, Higher Education Press, Beijing, p. 332.
- [5] Huang, C. (1997) *Rare Earth Coordination Chemistry (in Chinese)*, Science Press, Beijing.
- [6] Marks, T.J. and Fisher, R.D. (1979) *Organometallics of the f Element*, D. Reidel Publishing Company, Dordrecht.
- [7] Reisfeld, R. and Jorgensen, C.K. (1977) *Lasers and Excited States of Rare Earths*, Springer-Verlag, Berlin.
- [8] O’Laughlin, J.W. (1979) Chemical spectrophotometric and polarographic methods, in *Handbook on the Physics and Chemistry of Rare Earths*, Vol. **4**, Ch 37 (eds K.A. Gschneidner and L. Eyring), North-Holland Publishing Company, Amsterdam, pp. 341–376.
- [9] Buono-core, G.E., Li, H., and Marciniak, B. (1990) Quenching of excited states by lanthanide ions and chelates in solution. *Coordination Chemistry Reviews*, **99**, 55–87.
- [10] Yang, C., Fu, L.-M., Wang, Y. *et al.* (2004) Highly luminescent europium complex showing visible-light-sensitized red emission: direct observation of the singlet pathway. *Angewandte Chemie International Edition*, **43**, 5010–5013.
- [11] Bünzli, J.-C.G. and Eliseeva, S.V. (2010) Basics of lanthanide photophysics, in *Series on Fluorescence, Lanthanide Spectroscopy, Materials and Bio-Applications*, Vol. **7** (eds P. Hänninen and H. Härmä), Ch 2, Springer-Verlag, Berlin.
- [12] (a) Lemin, L., Jingqiang, R., and Guangxian, X. (1983) INDO studies on the electronic structure of lanthanide compounds. *International Journal of Quantum Chemistry*, **XXIII**, 1305–1316; (b) Jingqing, R. and Guangxian, X. (1986) Electronic structure and chemical bonding of the dimer of bis(η^5 -cyclopentadienyl)- ytterbium methyl. *International Journal of Quantum Chemistry*, **XXIX**, 1017–1024; (c) Jingqing, R. and Guangxian, X. (1987) INDO studies on the electronic structure and chemical bonding of a rare earth cluster compound, $\text{Gd}_{10}\text{C}_4\text{Cl}_{18}$. *Lanthanide and Actinide Research*, **2**, 67–78.
- [13] Chen, M., Wu, G., Huang, Z. *et al.* (1988) Studies on rare earth-indenyl compounds. 2. Synthesis and crystal structure of hexakis(tetrahydrofuran)sodium (μ -chloro)bis(triindenylneodymate). *Organometallics*, **7** (4), 802–806.
- [14] Ma, E., Yan, X., Wang, S. *et al.* (1981) The extraction chemistry of lanthanides with 2-ethyl-hexyle mono (2-ethyl-hexyle) phosphinate oxide. *Scientia Sinica B (in Chinese)*, **5**, 565–573.
- [15] Nugent, L.J. (1970) Theory of the tetrad effect in the lanthanide(III) and actinide(III) series. *Journal of Inorganic and Nuclear Chemistry*, **32**, 3485–3491.
- [16] Mullica, D.F. and Milligan, W.O. (1980) Structural refinement of cubic $\text{Lu}(\text{OH})_3$. *Journal of Inorganic and Nuclear Chemistry*, **42**, 223–227.
- [17] Peterson, E.J., Onstott, E.I., and Dreele, R.B.V. (1979) A refinement of cerium(III) trichloride heptahydrate in space group *P1*. *Acta Crystallographica*, **B35** (4), 805–809.
- [18] Fan, H., Liu, Y., Xu, G. *et al.* (1988) Synthesis and structure of diperchlorato-tetrakis (triphenyl phosphine oxide) neodymium mono-perchlorate complex containing one ethanol molecule of solvation. *Journal of Inorganic Chemistry (in Chinese)*, **4** (2), 9–20.
- [19] (a) Tanase, S. and Reedijk, J. (2006) Chemistry and magnetism of cyanido-bridged d-f assemblies. *Coordination Chemistry Reviews*, **250**, 2501–2510; (b) Ward, M.D. (2007) Transition-metal sensitized near-infrared luminescence from lanthanides in d-f heteronuclear arrays. *Coordination Chemistry Reviews*, **251**, 1663–1677.
- [20] Li, J., Huang, C., Xu, Z.H. *et al.* (1992) Studies on rare earth complexes of quaternary ammonium salt V. Crystal and molecular structure of tetrabutyl ammonium hexaaiso thiocyanato neodymium $[(\text{C}_4\text{H}_9)_4\text{N}]_3\text{Nd}(\text{NCS})_6$. *Journal of Inorganic Chemistry (in Chinese)*, **8** (1), 49–53.

- [21] Beall, G.W., Milligan, W.O., and Mroczkowski, S. (1976) Yttrium carbonate hydroxide. *Acta Crystallographica*, **B32** (11), 3143–3144.
- [22] Hansson, E. (1970) Structural studies on the rare earth carboxylates 5. The crystal and molecular structure of neodymium (III)oxalate 10.5-hydrate. *Acta Chemica Scandinavica*, **24**, 2969–2982.
- [23] Kahwa, I.A., Fronczek, F.R., and Selbin, J. (1984) The crystal and molecular structures of potassium- μ -oxalato-di [tris-oxalato-lanthanate(III)]-14-hydrates $K_8[Ox_3LnOxLnOx_3] \cdot 14H_2O$ [$Ln = Tb, Dy, Er, Yb, Y$]. *Inorganica Chimica Acta*, **82** (2), 167–172.
- [24] (a) Huang, C., Jin, X., Xu, G. *et al.* (1987) *Scientia Sinica*, **XXX** (8), 785–793; (b) Huang, C., Jin, T., Li, B. *et al.* Studies on extraction mechanism of the rare earth with quaternary ammonium salts. ISEC'86 International Solvent Extraction Conference, Munich, September 11–16, Vol. **II**, 215–221.
- [25] Mullica, D.F., Grossie, D.A., and Boatner, L.A. (1985) Coordination geometry and structural determinations of $SmPO_4$, $EuPO_4$ and $GdPO_4$. *Inorganica Chimica Acta*, **109** (2), 105–110.
- [26] Lindgren, O. (1977) The crystal structure of sodium cerium(III) sulfate hydrate, $NaCe(SO_4) \cdot H_2O$. *Acta Chemica Scandinavica*, **A31**, 591–594.
- [27] Lin, J., Wang, Y., Li, L. *et al.* (2005) Rare earth borates: an overview from the structural chemistry viewpoint, in *Inorganic Chemistry in Focus II* (eds G. Meyer, D. Naumann, and L. Wesemann), Wiley-VCH Verlag GmbH, Weinheim, Ch 16, pp. 293–378.
- [28] Li, L., Jin, X., Li, G. *et al.* (2003) Novel rare earth polyborates. 2. syntheses and structures. *Chemistry of Materials*, **15**, 2253–2260.

